OCT 1 8 1956
CLASSIFICATION cancelled

NACA RM A55I09

AERONAUTICS LIBRARY
California Institute of Technology

NACA

RESEARCH MEMORANDUM

FULL-SCALE WIND-TUNNEL TESTS OF A 35° SWEPTBACK WING AIRPLANE WITH HIGH-VELOCITY BLOWING OVER THE TRAILING-EDGE FLAPS

By Mark W. Kelly and William H. Tolhurst, Jr.

Ames Aeronautical Laboratory
Moffett Field, Calif.

CLASSIFIED DOCUMENT

This material contains information affecting the National Defense of the United States within the meaning of the espionage laws, Title 18, U.S.C., Secs. 793 and 794, the transmission or revelation of which in any manner to an unauthorized person is prohibited by law.

NATIONAL ADVISORY COMMITTEE
FOR AERONAUTICS

WASHINGTON

November 15, 1955

NATIONAL ADVISORY COMMITTEE FOR AERONAUTICS

RESEARCH MEMORANDUM

FULL-SCALE WIND-TUNNEL TESTS OF A 35° SWEPTBACK WING AIRPLANE WITH HIGH-VELOCITY BLOWING OVER THE TRAILING-EDGE FLAPS

By Mark W. Kelly and William H. Tolhurst, Jr.

SUMMARY

A wind-tunnel investigation was made to determine the effects of ejecting high-velocity air near the leading edge of plain trailing-edge flaps on a 35° sweptback wing. The tests were made with flap deflections from 45° to 85° and with pressure ratios across the flap nozzles from subcritical up to 2.9. A limited study of the effects of nozzle location and configuration on the efficiency of the flap was made. Measurements of the lift, drag, and pitching moment were made for Reynolds numbers from 5.8 to 10.1×10^6. Measurements were also made of the weight rate of flow, pressure, and temperature of the air supplied to the flap nozzles.

The results showed that blowing on the deflected flap produced large flap lift increments. The amount of air required to prevent flow separation on the flap was significantly less than that estimated from published two-dimensional data. When the amount of air ejected over the flap was just sufficient to prevent flow separation, the lift increment obtained agreed well with linear inviscid fluid theory up to flap deflections of 60°. The flap lift increment at 85° flap deflection was about 80 percent of that predicted theoretically. With larger amounts of air blown over the flap, these lift increments could be significantly increased. It was found that the performance of the flap was relatively insensitive to the location of the flap nozzle, to spacers in the nozzle, and to flow disturbances such as those caused by leading-edge slats or discontinuities on the wing or flap surface.

Analysis of the results indicated that installation of this system on an F-86 airplane is feasible.

INTRODUCTION

The trends of high-speed airplane design to high wing loadings and to configurations having low maximum usable lift coefficients have resulted in renewed interest in the application of boundary-layer control to attain high lift. Particular interest has been directed toward the application of boundary-layer control at the wing leading edge to delay the stall to higher angles of attack (ref. 1) and to the use of boundary-layer control on trailing-edge flaps to provide high lifts at low angles of attack (ref. 2). Two methods of applying boundary-layer control to trailing-edge flaps have been developed sufficiently to be considered for application to production aircraft. One method utilizes suction through a porous area near the flap leading edge, while the other utilizes a high-velocity air jet directed over the flap upper surface. These two installations are usually referred to as the area-suction flap and the blowing flap, respectively.

Flow separation is prevented on the area-suction flap by removing the low-energy portion of the boundary-layer air as it passes over the leading edge of the flap. Once flow separation has been eliminated, no further significant increases in lift are obtained by additional suction. It has been shown (ref. 2) that the lift increment produced with area suction depends on the quantity of boundary-layer air removed. The pumping power requirements of the area-suction flap are relatively low, since only a small amount of air must be removed from the flap and the pump pressure ratios required are not large.

Flow separation is prevented on the blowing flap by utilizing a high-velocity jet of air to re-energize the boundary layer as it passes over the leading edge of the flap (ref. 3). Unlike the area-suction flap, the blowing flap produces additional gains in lift when flows in excess of that required for attachment are used. The investigation of reference 3 indicated that the momentum of the air ejected over the flap determines the effectiveness of a blowing flap. If this concept is valid, then it should be possible to obtain the same aerodynamic performance from a blowing flap by using either high jet velocities and low mass-flow rates or low jet velocities and high mass-flow rates. This is a consideration of some importance, because it indicates that the flow and pressure requirements of a blowing flap are quite elastic and can be satisfied by many different pumping systems.

As pointed out in reference 3, a moderate amount of high-pressure air, which may be sufficient to satisfy the requirements of a blowing flap, can be bled from the compressor of a turbojet engine. However, since the engine performance deteriorates rapidly as the amount of bleed air is increased, it is important that the mass-flow requirements of the blowing flap be kept as low as possible. While the mass-flow requirements for a given jet momentum may obviously be minimized by using the highest possible

jet velocities, there is also the possibility that the mass-flow requirements may be further reduced by careful design of the flap itself, so that the jet momentum required to obtain the desired lift is decreased. Therefore, a preliminary, small-scale, two-dimensional test was made to investigate the effects of flap configuration on the momentum requirements of blowing flaps. Two models were used: One was a single-slotted flap arrangement with the nozzle located in the wing just ahead of the flap (such as that used in the investigation of ref. 3); the other was a plain flap configuration with the nozzle located on the upper surface of the flap near the point of minimum pressure. It was found that the momentum requirements of the plain flap were significantly less than those of the slotted flap. It was also found that the plain flap maintained its effectiveness to higher flap deflections than did the slotted flap. Comparison of data from other sources (refs. 4 and 5) show similar results in that the lift effectiveness and momentum requirements of slotted flaps (with blowing ahead of the slot) were generally improved when the slot was reduced or eliminated. It was therefore decided to further investigate a plain blowing-flap configuration on a swept wing at full-scale Reynolds numbers.

The purpose of this investigation was to provide full-scale, three-dimensional aerodynamic data for a swept-wing airplane having blowing flaps. It was also desired to obtain information which would enable application of the results to airplanes other than the particular one tested. In view of the fact that the most promising source of air for this type installation would be compressor bleed air from turbojet engines, and since a wide range of bleed-air pressures is available from various engines, special effort was made to determine whether the momentum of the air ejected over the flap was the sole parameter determining flap lift effectiveness over a relatively wide range of nozzle pressure ratios. Since each airplane incorporating blowing flaps will probably represent a different structural problem, this investigation included studies of the effects of nozzle location, discontinuities on the flap upper surface, and spacers in the nozzle itself. Finally, to further aid in generalization, an analysis was made which was directed at evaluating the accuracy of predictions of lift increments and momentum requirements which could be made from theory and two-dimensional data.

NOTATION

a	velocity of sound, ft/sec
A	area, sq ft
b	wing span, ft
c	wing chord parallel to plane of symmetry, ft

c_t horizontal-tail chord, parallel to plane of symmetry, ft

$\bar{c}$ mean aerodynamic chord, $\frac{2}{S}\int_0^{b/2} c^2 dy$

C_D drag coefficient, $\frac{\text{drag}}{q_o S}$

ΔC_D increment of drag coefficient due to flaps

C_L lift coefficient, $\frac{\text{lift}}{q_o S}$

ΔC_L increment of lift coefficient due to flaps

C_m pitching-moment coefficient, $\frac{\text{pitching moment}}{q_o S \bar{c}}$

ΔC_m increment of pitching-moment coefficient due to flaps

C_Q flow coefficient, $\frac{W_j}{w U_o S}$

C_μ momentum coefficient, $\frac{W_j/g}{q_o S} V_j$

$C_{L_{\delta_1}}$ rate of change of lift coefficient with flap deflection for full wing-chord flap (given as $C_{L_{\delta_1}}$ in ref. 6)

d distance from engine thrust line to moment center, positive when thrust line is above moment center, ft

$\frac{d\alpha}{d\delta_f}$ flap lift-effectiveness parameter

F_G gross thrust from engine, $\frac{W_E V_{TP}}{g}$, lb

F_N net thrust from engine, $F_G - \frac{W_E U_o}{g}$, lb

g acceleration of gravity, 32.2 ft/sec^2

h_s nozzle height, in.

M_j jet Mach number, $\frac{V_j}{a}$

p static pressure, lb/sq ft

p_t total pressure, lb/sq ft

p_d total pressure in flap duct, lb/sq ft

P_d duct pressure coefficient, $\frac{p_d - p_o}{q_o}$ for blowing, $\frac{p_o - p_d}{q_o}$ for suction

q dynamic pressure, lb/sq ft

R Reynolds number, $\frac{U_o \bar{c}}{\nu}$; or gas constant for air, 1715 sq ft/sec^2 ^oR

S wing area, sq ft

S_f wing area spanned by flaps, sq ft

T temperature, ^oR

U velocity, ft/sec

V_j jet velocity assuming isentropic expansion, $\sqrt{\frac{2\gamma}{\gamma - 1} RT_d \left[1 - \left(\frac{p_o}{p_d}\right)^{\frac{\gamma-1}{\gamma}}\right]}$, ft/sec

V_{TP} velocity at exit of engine tail pipe, ft/sec

W weight rate of flow, lb/sec

w specific weight of air at standard conditions, 0.0765 lb/cu ft

x distance along airfoil chord normal to wing quarter-chord line, in.

y spanwise distance perpendicular to plane of symmetry, ft

z height in inches above wing reference plane defined by quarter-chord line and the chord of the wing section at 0.663 b/2

Λ sweep angle, deg

α angle of attack of fuselage reference line, deg

δ_f flap deflection, measured normal to flap hinge line (given as $\underline{\delta}$ in ref. 6), deg

δ_f flap deflection, measured in a plane parallel to the plane of symmetry (given as δ in ref. 6), deg

ν kinematic viscosity of air, ft^2/sec

ϵ angle between engine tail pipe and fuselage reference line, deg ($+6.5^\circ$)

η pump efficiency

γ ratio of specific heats for air, 1.4

ρ mass density of air, slugs/cu ft

θ angular distance between flap nozzle and a line drawn through the flap hinge line perpendicular to the wing chord plane, (fig. 12)

Subscripts

BP conditions at engine compressor bleed ports

d trailing-edge flap duct

E engine

f trailing-edge flaps

i engine intake

j flap jet

o free stream

u uncorrected

TP engine tail pipe

2D two-dimensional

MODEL AND APPARATUS

Airplane

The model consisted of a YF-86D airplane on which the normal single-slotted flaps had been replaced by plain-type blowing flaps. A photograph showing the general arrangement of the airplane installed in the Ames 40- by 80-foot wind tunnel is presented in figure 1. The major dimensions and parameters of aerodynamic importance are shown in figure 2. The airfoil section at the wing root was an NACA 0012-64 (modified) and at the wing tip was an NACA 0011-64 (modified). The ordinates of the airfoil sections are given in table I. Detailed information for the wing and flaps is given in figure 3. Static-pressure orifices were installed in the after-portion of the flap upper surface so that the degree of flow separation could be estimated.

Flap Nozzles

The nozzle was essentially a slit in the flap upper surface extending over the full span of the flap. A section view of the nozzle is shown in figure 3. The nozzle blocks were machined from cold rolled mild steel stock and were fastened to the top wall of the flap duct with countersunk machine screws. Various nozzle heights were obtained by shimming the forward nozzle block. This assembly was made rigid enough to hold the nozzle deflections, under load, to acceptable values without the use of fasteners or spacers in the high-velocity portion of the nozzle. For part of the investigation, spacers were simulated by cementing small rectangular pieces of gasket material at regular intervals in the nozzle. Measurements of the height of the nozzle along the span of the flap are shown in figure 3(b) for the nozzle heights used in this investigation. It is seen that, even with the heavy nozzle construction utilized for the wind-tunnel model, the percent discrepancies in nozzle height are appreciable. Also presented in figure 3(b) are measurements taken with flow through the nozzle to show the change in nozzle height due to temperature and pressure effects.

In order to investigate the effects of chordwise location of the nozzle on the effectiveness of the flap, the flap duct was constructed so that it could be rotated about the flap hinge line independently of the flap itself. For most of the investigation the nozzle was located at an angular setting (θ) equal to one-half the flap deflection.

Engine and Ducting

For these tests, the J-47 turbojet engine normally used in the airplane was replaced by a modified J-34 engine. (This was done only because spare J-47 engines were not available.) The modifications to the J-34 consisted of (1) enlarging the compressor bleed ports so that larger quantities of air could be extracted from the engine compressor, (2) opening up the tail-pipe nozzle slightly to avoid higher than allowable tail-pipe temperatures when the engine was operated with large amounts of air bleed, and (3) replacing the compressor bleed-air manifold with larger ducting to handle the high flow rates with low pressure loss. The amount of air delivered to the flaps was controlled by a butterfly valve in each duct. The general arrangement of the modified engine mounted on a test stand is shown in figure 4. A sketch of the engine and ducting used in the airplane is shown in figure 5.

The weight rate of flow to each flap was obtained from total-pressure, static-pressure, and temperature measurements at stations 1 and 2. This system was calibrated using a thin plate orifice. The total-pressure and temperature measurements used for calculating the jet momentum were taken at the entrance to the flap duct (stations 3 and 4 in fig. 5). Static-pressure and temperature measurements were also made at the outboard end of the flap duct to obtain an estimate of the spanwise variation of the jet momentum.

TESTS

Range of Variables

The investigation covered a range of angles of attack from -2° to $+23^{\circ}$ and Reynolds numbers from 5.8 to 10.1×10^{6}. These Reynolds numbers were based on the mean aerodynamic chord of the airplane (8.08 ft) and correspond to free-stream dynamic pressures from 15 to 55 pounds per square foot. The range of flap deflections investigated was from 45° to 85°. The pressure ratio (p_d/p_o) furnished to the flap nozzles was varied from subcritical up to approximately 2.9 and the quantity flows were from 0 to 6.1 pounds per second. In order to utilize this range of pressure ratios the height of the flap nozzle was changed from approximately 0.065 inch to 0.016 inch. The airplane was tested with and without the horizontal tail, and with and without the leading-edge slats extended.

Method of Testing

To define completely the aerodynamic characteristics of the airplane as a function of flap jet momentum, it would have been necessary to obtain data for various jet momentum flows throughout the angle-of-attack range. However, in order to expedite the tests, the momentum flow was varied at only three angles of attack, 0°, 8°, and 12°. (The angle of attack for maximum lift with leading-edge slats retracted was near 12°.) The additional information required to obtain typical lift, drag, and pitching-moment data for the airplane was obtained by testing at several other angles of attack with a constant jet momentum well above that required for flow attachment.

Measurement of Engine Thrust

Since a turbojet engine mounted in the fuselage was used as the source of high-pressure air for the flap nozzles, it was necessary to correct the measured force data for the effects of engine thrust. The engine thrust was obtained from both a static-thrust calibration using the wind-tunnel balance system, and from total- and static-pressure measurements at the engine inlet and tail-pipe nozzle. Gross thrust was obtained from the tail-pipe total-pressure measurements by the use of the following equation:

$$F_G = CA_{TP}p_{TP}\frac{2\gamma}{\gamma - 1}\left[\left(\frac{p_t}{p}\right)_{TP}^{\frac{\gamma-1}{\gamma}} - 1\right]$$

The coefficient C was determined by solving for C in the above equation with values of F_G obtained from the static-thrust calibration. The net thrust of the engine was obtained by subtracting the ram drag from the gross thrust.

$$F_N = F_G - \frac{(W_E)(U_o)}{g}$$

The weight rate of flow through the engine, W_E, was obtained from the pressure measurements at the engine compressor intake by the following equation:

$$W_E = A_i\sqrt{\frac{2\gamma}{\gamma - 1}\frac{(gp_i)^2}{RT_i}\left[\left(\frac{p_t}{p}\right)_i^{\frac{\gamma-1}{\gamma}} - 1\right]}$$

Values of engine net thrust obtained from the static-thrust calibration and from the pressure measurements were in good agreement (±2 percent).

CORRECTIONS

Effects of Engine Thrust

The force data obtained from the wind-tunnel balance system were corrected for the effects of engine thrust as follows:

$$C_L = \frac{\text{total lift}}{q_o S} - \frac{F_N}{q_o S} \sin(\alpha + \epsilon)$$

$$C_D = \frac{\text{total drag}}{q_o S} + \frac{F_N}{q_o S} \cos(\alpha + \epsilon)$$

$$C_m = \frac{\text{total moment}}{q_o S \bar{c}} + \frac{F_N d}{q_o S \bar{c}}$$

The force due to turning the engine air at the inlet is not accounted for in these corrections, since computations indicated that this force was negligible.

Effects of Wind-Tunnel-Wall Interference

The following corrections for tunnel-wall effects were made:

$$\alpha = \alpha_u + 0.611\ C_{L_u}$$

$$C_D = C_{D_u} + 0.0107\ C_{L_u}{}^2$$

$$C_m = C_{m_u} + 0.00691\ C_{L_u} \text{ (for tail-on tests only)}$$

RESULTS AND DISCUSSION

Typical Aerodynamic Characteristics

Correlation of momentum coefficient with blowing-flap performance.- One of the first objectives of the test program was to establish whether the effectiveness of a particular blowing-flap configuration was determined

solely by the momentum of the air ejected over the flap. This was done by making a series of tests on the same basic flap configuration with various nozzle openings. Typical results of these tests are presented in figure 6(a). It should be noted that, although the nozzle opening was changed from a value of 0.016 inch to 0.065 inch (corresponding to values of h_s/c from 0.00017 to 0.00067), good correlation with momentum coefficient is obtained. The data presented in figure 6(a) cover a range of nozzle pressure ratios from subcritical up to 2.9, and therefore a range of expanded jet velocities from subsonic to supersonic. It should be noted that no particular aerodynamic difficulties or benefits are associated with either subsonic or supersonic jet velocities, at least within the range of pressure ratios available for these tests. Corresponding variations of lift coefficient with flow coefficient and duct pressure coefficient are shown in figures 6(b) and 6(c), respectively. Here it is seen that the effects of nozzle height are significant, and that values of flow coefficient or pressure coefficient are meaningless unless the nozzle height is specified. While the data presented in figure 6 are for 0° angle of attack only, similar results were obtained at 8° and 12° angle of attack. Thus, within the limits of this investigation, it appears that blowing-flap effectiveness on swept wings is determined by the momentum of the air ejected over the flap. This same result was obtained in the two-dimensional investigation of reference 3. However, as pointed out in reference 5, this degree of correlation with momentum coefficient has not always been obtained in other investigations, particularly those using low-pressure air where the jet velocity is of the same order of magnitude as the free-stream velocity.

Typical effects of blowing on lift, drag, and pitching-moment characteristics.- Figure 7 presents the tail-off lift, drag, and pitching-moment characteristics of the airplane with various flap deflections with and without blowing. (All data presented in this report were obtained with the leading-edge slats in and locked and the tail off unless otherwise specified.) The data obtained with blowing were taken at constant values of momentum coefficient which were more than sufficient to provide attached flow for each flap deflection. It is seen that blowing over the flap produced the type of lift and pitching-moment increments which would be expected from substantial increases in flap effectiveness. The drag coefficient for a given flap deflection was increased by blowing. This may be surprising in view of the fact that blowing over the flap should reduce the amount of flow separation and hence the profile drag of the flap. However, it must be remembered that the total airplane drag is the sum of both profile and induced drag. Since the total drag was increased by blowing, while the profile drag was decreased, it must be concluded that blowing over the flaps resulted in an increase in induced drag. The use of a short span, highly effective flap will always cause a significant distortion of the wing span loading and a resulting increase in the induced drag of the wing. The order of magnitude of this induced drag can be estimated from the theory of reference 6. It should be noted that this induced drag increment is a function of flap span and is more for small span flaps than it is for large span flaps.

The data presented in figure 7 were obtained with the flap nozzle located at an angular setting (θ) equal to one-half the flap deflection, as previously pointed out in the section "MODEL AND APPARATUS." This was done because previous research (ref. 2) had indicated that this setting would put the nozzle near the minimum-pressure point on the flap, and this was believed to be near the optimum location. Subsequent testing to determine the effects of nozzle location (see the section entitled "Nozzle location," p. 14) indicated that this location was, in fact, near the optimum. However, the flap was relatively insensitive to nozzle position and the data presented in figure 7 are typical of those which would be obtained with the nozzle located anywhere between the minimum-pressure point on the flap and the wing-flap juncture.

Figures 7(b), (c), and (d) present the variation of lift, drag, and pitching-moment coefficient with momentum coefficient. As mentioned previously, the momentum coefficient was varied only at uncorrected angles of attack of 0°, 8°, and 12°. (The momentum coefficient was not varied at 12° angle of attack for flap deflections of 75° and 85° since, with these flap deflections, the wing had already passed maximum lift.) Figure 7(b) shows that, as the momentum coefficient was increased, the lift at first increased rapidly but then the rate of increase fell off to a relatively low value. Static-pressure measurements on the upper surface of the flap indicated that the initial rapid increase in lift was associated with the control of the boundary layer on the flap. The additional lift obtained after the flow was attached was probably associated with an increase in wing circulation induced by the jet flow over the flap. The exact nature of this phenomenon is not completely understood at this time.

The data presented in figure 7(b) indicate that the momentum coefficient required for a given flap lift increment is relatively low when the flap deflection is large enough so that the desired lift is obtained by using blowing primarily for boundary-layer control rather than to provide jet-induced circulation. However, there may be applications where the required momentum coefficient is not critical, but where either the drag or pitching-moment increase associated with increased flap effectiveness is critical. Figure 8(a), cross-plotted from figure 7(c), shows the drag coefficients associated with given lift coefficients at 0° uncorrected angle of attack for various flap deflections. It is seen that minimum drag for a given lift coefficient is obtained when the smaller flap deflections are used with sufficiently large momentum coefficients. However, if these momentum coefficients are obtained by bleeding air from turbojet engines, the use of large momentum coefficients will generally result in high thrust loss from the engine. Since it is usually thrust minus drag which is of concern, the selection of the proper flap deflection and momentum coefficient for a particular application will entail an analysis of both the aerodynamics of the blowing flap and the thrust versus bleed-air characteristics of the engine being used. Figure 8(b) presents a similar plot of pitching-moment coefficient against momentum coefficient for a given lift coefficient at 0° angle of attack. This plot indicates that

the minimum pitching moment is obtained with the higher flap deflections. However, the margin of superiority shown in most cases is not large and, in view of the scatter of the pitching-moment data, is not believed to be very significant. It might be noted that the pitching moment per unit lift due to flap deflection is not significantly changed by blowing. This is shown in the following table which was obtained from the data presented in figures 7(b) and 7(d) for 0° uncorrected angle of attack:

δ_f	45°		60°		75°		85°	
C_μ	0	0.006	0	0.0105	0	0.0168	0	0.0255
$\frac{\Delta C_m}{\Delta C_L}$	-.20	-.18	-.20	-.18	-.18	-.17	-.16	-.17

Effects of Reynolds number.- The variation of lift coefficient with momentum coefficient for Reynolds numbers from 5.8 to 10.1×10^6 is shown in figure 9. It is seen that no significant effect of Reynolds number on the lift increment due to blowing was obtained.

Effects of leading-edge slats.- Figures 10(a) and (b) show the effects of extending the leading-edge slats on the aerodynamic characteristics of the airplane with and without blowing on the flaps. It is seen that extending the slats had no significant effect on the flap performance, that is, had no effect on the lift increment due to blowing or the required momentum coefficients. The loss in lift at angles of attack below maximum lift is due primarily to the nose camber effect of the slats. It should be noted that there is no nonlinearity in the lift curve such as that obtained with area-suction flaps in the investigation of reference 2, where the vortex shed from the slat root spoiled the flow over a portion of the flap. The leading-edge slats did not provide a significant increase in maximum lift, although they did change the type of stall from one that was very abrupt to one that was relatively gentle. The pitching-moment data show that, with blowing on, the leading-edge slats did not provide the stable variation in pitching moment at the stall that was obtained without blowing.

Effect of horizontal tail.- Lift, drag, and pitching-moment data for the airplane with and without the horizontal tail and with and without blowing on the flap are shown in figure 11. It is seen that with the tail on and at a constant lift coefficient, blowing over the flap produced a positive pitching-moment change. This was caused by an increase in downwash, and possibly dynamic pressure, in the vicinity of the horizontal tail.

Effects of Nozzle and Flap Configuration on Flow Requirements

Nozzle location.- Figure 12(a) presents lift coefficient as a function of momentum coefficient for the airplane with flaps deflected 60° having various nozzle locations. The data indicate that, for the range of nozzle locations available with the flaps deflected 60°, no appreciable effect of nozzle location was found at angles of attack of 8° and 12°, which are in the range of most significance as far as landing and take-off of the airplane is concerned. Figure 12(b) presents similar data with the flaps deflected 85°. Here it was possible to move the nozzle far enough downstream on the flap so that the flow could not be attached with any value of momentum coefficient available. In general, these data indicate that, as long as the nozzle is located between the wing-flap juncture and the minimum-pressure point on the flap, no significant effect on flow requirements will be obtained. It should be noted that, for the case where the nozzle is fixed with respect to the flap, the nozzle should be positioned approximately at the location of the minimum-pressure point on the flap for the maximum flap deflection contemplated. At lower flap deflections the nozzle will then be ahead of the minimum-pressure point on the flap and satisfactory performance should be obtained.

Effect of spacers in nozzle.- For this phase of the investigation the nozzle was plugged at regular spanwise intervals to simulate an interrupted nozzle, that is, several discrete nozzles along the flap span. Data for various nozzle configurations are presented in figure 13. It is seen that no significant effect was obtained until nozzles 2 inches long separated by 1-inch spacers were simulated. For this arrangement, it was found that the required momentum coefficient for a given lift coefficient was somewhat increased.

Effect of discontinuities on flap.- Figure 14 shows the variation of lift coefficient with momentum coefficient when a full-span step discontinuity was placed on the flap upper surface to simulate conditions that might be encountered on a production installation. It was found that the effect of these surface discontinuities was relatively small. However, it is expected that these effects would become more serious, if the break in the upper surface were moved closer to the nozzle.

Comparison With Theory and Two-Dimensional Data

The lift increment obtained by blowing over the flaps is caused by two fundamentally different phenomena: boundary-layer control and circulation control. The boundary-layer control effect dominates at low momentum coefficients and is typified by a relatively rapid increase in lift coefficient with increasing momentum coefficient. After flow separation

has been essentially eliminated, the effect of circulation control becomes more pronounced and is characterized by a gradual and nearly linear increase in lift coefficient with increasing momentum coefficient. While it is not always possible experimentally to separate these two effects completely, it is convenient for the purpose of analysis to attempt to identify (1) the lift increment due to boundary-layer control, (2) the momentum coefficient required for boundary-layer control, and (3) the lift increment due to circulation control.

Lift increment due to boundary-layer control.- Usually any large discrepancies between the lift of a wing and that predicted from inviscid fluid theory can be attributed to flow separation. Since the application of boundary-layer control should reduce the amount of flow separation, it is reasonable to assume that the lift obtained by the use of boundary-layer control should approximate that predicted by inviscid fluid theory. Figure 15 shows a comparison of the flap lift increments due to boundary-layer control obtained in this investigation with those estimated by the theory of reference 6.[1] The experimental flap lift increments chosen were those existing when the flow over the flap first became attached, as indicated by static-pressure measurements near the flap trailing edge. (The last pressure orifice was at approximately 98 percent chord.) The momentum coefficients required to eliminate flow separation for each flap deflection are also presented. It may be seen by referring to figure 7(b) that these momentum coefficients are in the region where the rate of increase of lift coefficient with momentum coefficient falls off to a relatively low value. This affords an alternative, but often less precise, method of selecting the point of flow attachment. It may be seen from figure 15 that, for flap deflections up to 60°, the estimated and experimental flap lift increments are in good agreement. The discrepancies between the predicted and experimental values at higher flap deflections are believed to be due

---

[1]The theoretical flap effectiveness was estimated from

$$\Delta C_L = \left(\frac{d\alpha}{d\delta_f}\right) C_{L\underline{\delta}_1} \frac{\underline{\delta}_f}{57.3} \quad \text{(equivalent to eq. 7, ref. 6)}$$

For the F-86D wing

$$C_{L\underline{\delta}_1} = 1.52 \text{ (from cross plot of fig. 5, ref. 6)}$$

$$\frac{d\alpha}{d\delta_f} = 0.58 \text{ (from curve for theoretical flap effectiveness, fig. 3, ref. 6. Average } c_f/c = 0.23 \text{ perpendicular to flap hinge line)}$$

$$\tan \underline{\delta}_f = \cos \Lambda_f \tan \delta_f = 0.895 \tan \delta_f$$

$$\Delta C_L = \frac{(0.58)(1.52)}{57.3} \underline{\delta}_f = 0.0154 \underline{\delta}_f$$

---

more to the linearizing assumptions utilized in the theory rather than to an actual deterioration of the flow over the flap. Even at a flap deflection of 85° the static-pressure measurements on the flaps indicated that attached flow was obtained.

It should be noted that, when the theory of reference 6 is used, the flap effectiveness parameter, $d\alpha/d\delta$, may be determined either from two-dimensional theory or from two-dimensional experimental results. In the foregoing analysis, the value of $d\alpha/d\delta$ was computed from two-dimensional thin-airfoil theory. An effort was made to substantiate the use of this theoretical value by comparing available two-dimensional experimental results with those estimated by thin-airfoil theory. It was realized at the outset that thin-airfoil theory could not account for all factors determining flap effectiveness. However, it was believed that such a comparison would help to correlate the lift increments due to boundary-layer control obtained from the various two-dimensional investigations. Such a correlation would provide a basis for the use of two-dimensional data for estimating the lift increments of blowing-flap installations on various wing designs. It was found, however, that this correlation could not readily be made with existing two-dimensional data. For example, the experimental flap lift increments due to boundary-layer control obtained from two-dimensional tests in various facilities were from 0 to 30 percent below the values estimated from thin-airfoil theory (refs. 3, 4, and 5). The reasons for these differences are not completely understood at the present time. However, since nearly theoretical flap lift increments have been obtained in some of the two-dimensional investigations, and in view of the comparisons shown in figure 15 for the three-dimensional case, it is believed that the theory of reference 6 should, with $d\alpha/d\delta$ obtained from two-dimensional thin-airfoil theory, give realistic predictions of the lift increment due to boundary-layer control.

Momentum coefficient required for boundary-layer control.- At the present time, no theoretical method exists for predicting the momentum coefficient required to prevent separation of a turbulent boundary layer in an adverse pressure gradient. Therefore, an empirical approach using experimental data is the only available means of estimating the momentum-coefficient requirements of blowing flaps. Since most of the existing data for blowing flaps are from two-dimensional investigations, some method of applying these data to three-dimensional wings would be desirable. One method that has been used for this purpose consists of a design procedure similar to that outlined in Appendix A of reference 2.[2] This method has

[2]This procedure may be stated mathematically as

$$\text{Equivalent } C_{\mu_{2D}} = \frac{C_\mu}{\left(\frac{S_f}{S}\right)\cos^2\Lambda_f}$$

For the wing of this investigation

$$\text{Equivalent } C_{\mu_{2D}} = \frac{C_\mu}{(0.39)(0.895)^2} = 3.20\ C_\mu$$

been used to obtain the relationship between the three-dimensional values of C_μ required for flow attachment (from fig. 15) and the "equivalent" two-dimensional values based on the component of the stream velocity perpendicular to the hinge line of the flap and the area of the wing spanned by the flaps. The results for the several flap deflections are as follows:

Flap deflection, deg	C_μ, three-dimensional	Equivalent C_μ, two-dimensional
45	0.006	0.019
60	.0105	.034
75	.0168	.054
85	.0255	.082

The above-listed values of equivalent two-dimensional C_μ's are about 60 to 75 percent of those obtained from the small-scale, two-dimensional investigation described in the introduction to this report. This could possibly be accounted for by differences between the two-dimensional flap configuration[3] and that used in the three-dimensional tests, or by the low Reynolds number ($R = 1.66 \times 10^6$) of the two-dimensional investigation. It is also possible that the spanwise boundary-layer flow on the swept wing or some other three-dimensional effect makes the above simplified procedure inadequate. It might also be noted that the equivalent two-dimensional C_μ requirements computed from the data of this investigation are considerably below those required on the best two-dimensional arrangements for which published data are available (refs. 3, 4, and 5).

Lift increment due to circulation control.- There is no theoretical procedure available at the present time for estimating the circulation control effect obtained by blowing over the flaps. Examination of available two-dimensional data (refs. 3, 4, and 5) indicates that after the flow over the flap is attached, the value of dC_L/dC_μ is usually between 4 and 8. Comparable values obtained from this investigation are from 6 to 7. From a practical viewpoint, an accurate estimate of this portion of the lift increment is probably not required. For most airplane installations in the near future, the limited momentum coefficients available will probably restrict the lift due to circulation control to a small percentage of the total lift increment.

Comparison With Area-Suction Flaps

Since the basic wing of the model used in the investigation of area-suction flaps reported in reference 2 was the same as that used in this

[3]The two-dimensional model used a 32-percent-chord flap which was pivoted about a point on the wing-chord plane.

investigation, it is possible to obtain a fairly reliable comparison of the characteristics of these two types of boundary-layer control. However, in making this comparison, the following differences in model configuration should be noted: (1) the flap chord of the area-suction flap was larger than that of the blowing flap, (2) the hinge line of the area-suction flap was farther aft than that of the blowing flap, and (3) the fuselages used were quite dissimilar.

Flap lift increment.- Figure 16(a) shows a comparison of lift increments obtained from the area-suction and blowing flaps at 0° angle of attack. The lift increments for the blowing flap were chosen, as in figure 15, at momentum coefficients for which the flow on the flap first became attached. The lift increments for the suction flap were correspondingly chosen near the critical flow coefficient. It is seen that below flap deflections of 60° the lift increments obtained from the two flaps are comparable, but above 60°, the blowing flap appears to be more effective than does the area-suction flap. A point worth noting when considering the above comparison is that larger differences in the lift increments would occur if the suction and blowing flow quantities were not limited to those required for flow attachment.

The maximum lift coefficient obtained from the model with area-suction flaps was 1.68. (See fig. 10(a) of ref. 2, data for the model with F-86A leading-edge configuration and 55° flap deflection.) The maximum lift coefficient obtained from the airplane with blowing flaps deflected 55° was about 1.70. With either suction or blowing flaps, maximum lift was determined primarily by flow separation at the wing leading edge. Extending the leading-edge slats did not give a significant increase in maximum lift for either the area-suction or blowing-flap configuration.

Flow and pressure requirements.- A comparison of the variation of lift coefficient with flow coefficient for the two flaps is shown in figure 16(b). For this comparison, data for the blowing flap with a nozzle height of 0.03 inch was used since computations (presented in the next section) indicated that this was approximately the nozzle height which would be used on an F-86 airplane installation. As mentioned previously, lower flow coefficients would produce the same lift coefficient for the blowing flap if smaller nozzles were used. However, the pressure ratios required would be correspondingly larger. In order to make a more valid comparison between the suction and blowing flaps, the blowing flap was tested with a chord extension which gave a chord equal to that of the suction flap. Data for this configuration are also shown in figure 16(b). Data for two area-suction flap configurations having different porous materials are presented. The curve for the area-suction flap with a porous material of constant thickness was obtained from figure 11 of reference 2. The data for the area-suction flap with a porous material of variable thickness has not been previously published in this form but is discussed in Appendix B of reference 2.

A comparison of the variation of lift coefficient with duct pressure coefficient for the two flaps is shown in figure 16(c). Again, data for the blowing flap with a nozzle height of 0.03 inch are presented. It is seen that the pressure requirements for the blowing flap with this nozzle are much higher than those for the area-suction flaps.

On applications for which it is intended to use turbine-engine compressor air bleed to furnish the air required by the boundary-layer control system, it is well to note that, for the blowing flap, the amount of air required by the flap is equal to that taken from the engine; however, for the area-suction flap this is not necessarily the case. Here the amount of air which must be extracted from the engine is determined by the pumping power needed to remove the required amount of air from the flap. The pumping power requirements of the area-suction flap are given by

$$hp = \frac{R}{550g}\left(\frac{\gamma}{\gamma - 1}\right) W_f T_o \left[1 - \left(\frac{p_d}{p_o}\right)^{\frac{\gamma-1}{\gamma}}\right]$$

If compressed air from the engine compressor bleed system is used as the power source for the pump, then the power output of the pump is

$$hp = \frac{\eta R}{550g}\left(\frac{\gamma}{\gamma - 1}\right) W_{BP} T_{BP} \left[1 - \left(\frac{p_o}{p_{BP}}\right)^{\frac{\gamma-1}{\gamma}}\right]$$

where η is the efficiency of the pump. The amount of engine bleed air required is determined by matching the output of the pump to the power requirements of the flap. This gives

$$W_{BP} = \frac{W_f}{\eta}\frac{T_o}{T_{BP}}\left[\frac{1 - \left(\frac{p_d}{p_o}\right)^{\frac{\gamma-1}{\gamma}}}{1 - \left(\frac{p_o}{p_{BP}}\right)^{\frac{\gamma-1}{\gamma}}}\right]$$

Application of this equation to the F-86 airplane flying at 120 knots with 75-percent engine rpm ($T_{BP} = 750^\circ$ R, $p_{BP}/p_o = 3$) indicates that the ratio of engine bleed-air requirements to flap suction-air requirements would be about 0.46 if ejector pumps having efficiencies of 15 percent were used. If an air turbine driven pump having an over-all efficiency of 60 percent were used, this ratio would decrease to about 0.12.

In summary, these comparisons indicate that, at the same flap deflection, the lift increment due to boundary-layer control of the blowing flap is larger than that of the area-suction flap. This difference in lift may be increased if sufficient air is available to provide the blowing flap

with large values of momentum coefficient. The power requirements of the area-suction flaps are considerably less than those of the blowing flaps. In aircraft installations where the source of power is compressed air from a turbojet-engine bleed-air system, these low power requirements result in low bleed-air requirements and correspondingly low engine thrust losses for operation of the area-suction flap. In general, it is believed that, for a particular airplane the choice between these two boundary-layer control systems will depend primarily upon the engine thrust loss, space available for ducting, and weight penalties rather than the differences in their aerodynamic characteristics.

Application of Results to an F-86 Airplane

Figure 17 presents an application of the results of this investigation to an F-86 airplane having a J-47 engine. This plot shows the weight rate of flow versus pressure-ratio characteristics of the blowing flap, the engine bleed-air system, and various sizes of flap nozzles. The hyperbolic-shaped solid curves represent the weight rate of flow and pressure ratio required to give a momentum coefficient of 0.012 at flight speeds of 100, 120, and 140 knots. This is approximately 14 percent above the momentum coefficient required for flow attachment on the flap deflected 60°. These curves were developed from the equation

$$W_{BP} = \frac{C_\mu g q_o S}{M_j \left(\frac{a_j}{a_d}\right) \sqrt{\gamma R T_d}}$$

where M_j and a_j/a_d are obtained as functions of pressure ratio from isentropic flow relationships, and the duct temperature, T_d, is obtained from temperature- versus pressure-ratio characteristics of the engine bleed-air system. The weight rate of flow and pressure ratios available from compressor air bleed on the J-47 engine at various engine speeds are shown as dashed lines in figure 17. (It should be noted that the pressure ratios given here are those existing at the engine compressor bleed ports. The pressure available at the flap nozzle will, of course, depend on the duct losses of the particular installation.) The thrust losses associated with extracting this air from the engine and the conditions where the allowable tail-pipe temperature will be exceeded are also shown. It is seen that, to obtain the specified momentum coefficient for this range of flight speeds, the loss in engine thrust will be approximately 3 to 7 percent. The allowable tail-pipe temperature will not be exceeded for engine speeds below 98-percent rpm for the maximum value of air bleed considered here. To aid in the selection of the proper flap nozzle size, the weight rate of flow which can be driven through various nozzles was computed and

is represented in figure 17 by the nearly linear broken lines. These curves were developed from the equation

$$W_j = g\rho_d a_d \left(\frac{\rho^*}{\rho_d}\right)\left(\frac{a^*}{a_d}\right)A_j$$

where $(\rho^*/\rho_d) = 0.6339$ and $(a^*/a_d) = 0.9129$ for air flow in choked nozzles. The quantities ρ_d and a_d were evaluated for air having the pressure and temperature conditions existing at the engine compressor bleed ports. It is seen that, if it is desired to have the flap fully effective for landing approach conditions (about 100 to 120 knots and 70- to 80-percent rpm), a nozzle height of 0.02 to 0.03 inch should be used. For this arrangement the loss of engine thrust will be about 4 or 5 percent. However, if this same nozzle were used under take-off conditions, the thrust loss would be about 8 percent unless a throttle valve were used to decrease the flap duct pressure to values near those obtained for the landing approach condition. It should be noted that the selection of 60° flap deflection was made arbitrarily for the purpose of this example. It is likely that a lower flap deflection would prove more satisfactory for take-off, since both the drag and engine thrust loss would be less. However, for any flap deflection up to 60°, these computations indicate that a blowing-flap installation on the F-86 airplane would produce large flap lift increments, and that the thrust loss from the engine would not be prohibitive.

CONCLUSIONS

The following conclusions have been made from analysis of the results of this investigation:

1. Good correlation of blowing-flap effectiveness with momentum coefficient is obtained for blowing-flap installations in the range of jet-to-free-stream velocity ratios covered in this investigation.

2. The momentum coefficient required for flow attachment on the blowing flap used for this investigation is significantly less than that estimated from available two-dimensional data.

3. The lift increment obtained by preventing flow separation on the flap can be predicted up to 60° flap deflection by the linear inviscid fluid theory of reference 6.

4. Higher lift increments than those obtained by preventing flow separation on the flap can be achieved by increasing the momentum coefficient to values in excess of that required for flow attachment. However, these same lift increments can generally be obtained with lower momentum

coefficients by using larger flap deflections with blowing utilized primarily for boundary-layer control, rather than to provide jet-induced circulation.

5. For flap deflections up to 60°, the flap nozzle can be located on the upper surface anywhere between the minimum-pressure point on the flap and the wing-flap juncture without seriously affecting the flap effectiveness. If the flap nozzle is moved too far downstream of the minimum-pressure point, a serious loss in flap effectiveness may result.

6. The blowing flap is relatively insensitive to spacers or structural members in the nozzle throat. It is also insensitive to flow disturbances such as those obtained from leading-edge slats or from discontinuities on the surface of the wing or flap.

7. The blowing flap of this investigation retains its effectiveness to higher flap deflections than does the area-suction flap of the investigation reported in reference 2. At the same flap deflection, the blowing flap can produce significantly higher lift increments than the area-suction flap if momentum coefficients in excess of that required to prevent flow separation on the flap are available. If applied to the F-86 airplane, the blowing flap will require slightly higher flow coefficients and much higher duct pressure coefficients than the area-suction flap. In general, it is believed that the lift, drag, and pitching-moment characteristics associated with each of these means of boundary-layer control are similar enough that, for a particular airplane, the choice between the two systems will depend primarily on such factors as available pumping capacity and space and ducting limitations, rather than their aerodynamic characteristics.

8. Application of the results of this investigation to an analysis of a blowing-flap installation on an F-86 airplane having a J-47 turbojet engine indicates that such an installation is practicable.

Ames Aeronautical Laboratory
National Advisory Committee for Aeronautics
Moffett Field, Calif., Sept. 9, 1955

REFERENCES

1. Holzhauser, Curt A., and Martin, Robert K.: The Use of Leading-Edge Area Suction to Increase the Maximum Lift Coefficient of a 35° Swept-Back Wing. NACA RM A52G17, 1952.

2. Cook, Woodrow L., Holzhauser, Curt A., and Kelly, Mark W.: The Use of Area Suction for the Purpose of Improving Trailing-Edge Flap Effectiveness on a 35° Sweptback Wing. NACA RM A53E06, 1953.

3. Harlkeroad, E. L., and Murphy, R. D.: Two-Dimensional Wind Tunnel Tests of a Model of an F9F-5 Airplane Wing Section Using a High-Speed Jet Blowing Over the Flap. Part I - Tests of a 6-Foot Chord Model. DTMB Rep. Aero 845, BuAer, Navy Dept., TED TMB DE-3134, May 1953.

4. Wallace, Richard E., and Stalter, J. L.: Systematic, Two-Dimensional Tests of an NACA 23015 Airfoil Section with a Single-Slotted Flap and Circulation Control. Aerodynamic Rep. No. 120, Municipal University of Wichita, Aug. 1954.

5. Williams, J.: An Analysis of Aerodynamic Data on Blowing Over Trailing Edge Flaps for Increasing Lift. British ARC Performance Subcommittee 17,027, Sept. 6, 1954.

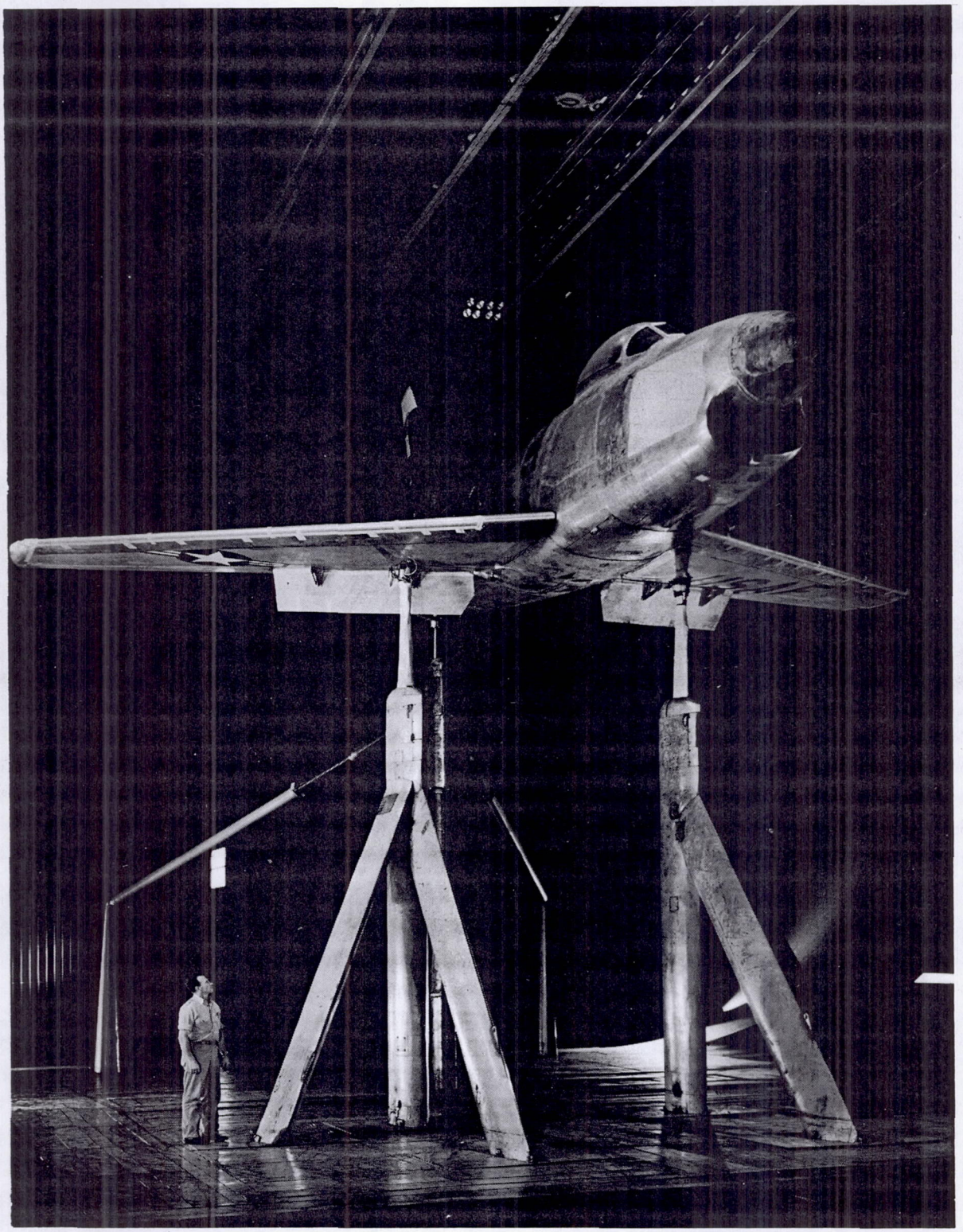
6. DeYoung, John: Theoretical Symmetric Span Loading Due to Flap Deflection for Wings of Arbitrary Plan Form at Subsonic Speeds. NACA Rep. 1071, 1952. (Formerly NACA TN 2278)

TABLE I.- COORDINATES OF THE WING AIRFOIL SECTIONS NORMAL TO THE WING QUARTER-CHORD LINE AT TWO SPAN STATIONS

[Dimensions given in inches]

Section at 0.467 semispan			Section at 0.857 semispan		
x	z		x	z	
	Upper surface	Lower surface		Upper surface	Lower surface
0	0.231	---	0	-0.098	---
.119	.738	-0.307	.089	.278	-0.464
.239	.943	-.516	.177	.420	-.605
.398	1.127	-.698	.295	.562	-.739
.597	1.320	-.895	.443	.701	-.879
.996	1.607	-1.196	.738	.908	-1.089
1.992	2.104	-1.703	1.476	1.273	-1.437
3.984	2.715	-2.358	2.952	1.730	-1.878
5.976	3.121	-2.811	4.428	2.046	-2.176
7.968	3.428	-3.161	5.903	2.290	-2.401
11.952	3.863	-3.687	8.855	2.648	-2.722
15.936	4.157	-4.064	11.806	2.911	-2.944
19.920	4.357	-4.364	14.758	3.104	-3.102
23.904	4.480	-4.573	17.710	3.244	-3.200
27.888	4.533	-4.719	20.661	3.333	-3.250
31.872	4.525	-4.800	23.613	3.380	-3.256
35.856	4.444	-4.812	26.564	3.373	-3.213
39.840	4.299	-4.758	29.516	3.322	-3.126
43.825	4.081	-4.638	32.467	3.219	-2.989
47.809	3.808	-4.452	35.419	3.074	-2.803
51.793	3.470	-4.202	38.370	2.885	-2.574
55.777	3.066	-3.891	41.322	2.650	-2.302
59.761	2.603	-3.521	44.273	2.374	-1.986
[a]63.745	2.079	-3.089	[a]47.225	2.054	-1.625
83.681	-.740	---	63.031	.321	---
L.E. radius: 1.202, center at 1.201, 0.216			L.E. radius: 0.822, center at 0.822, -0.093		

[a]Straight lines to trailing edge



A-19719

Figure 1.- Photograph of the YF-86D airplane mounted in the Ames 40- by 80-foot wind tunnel.

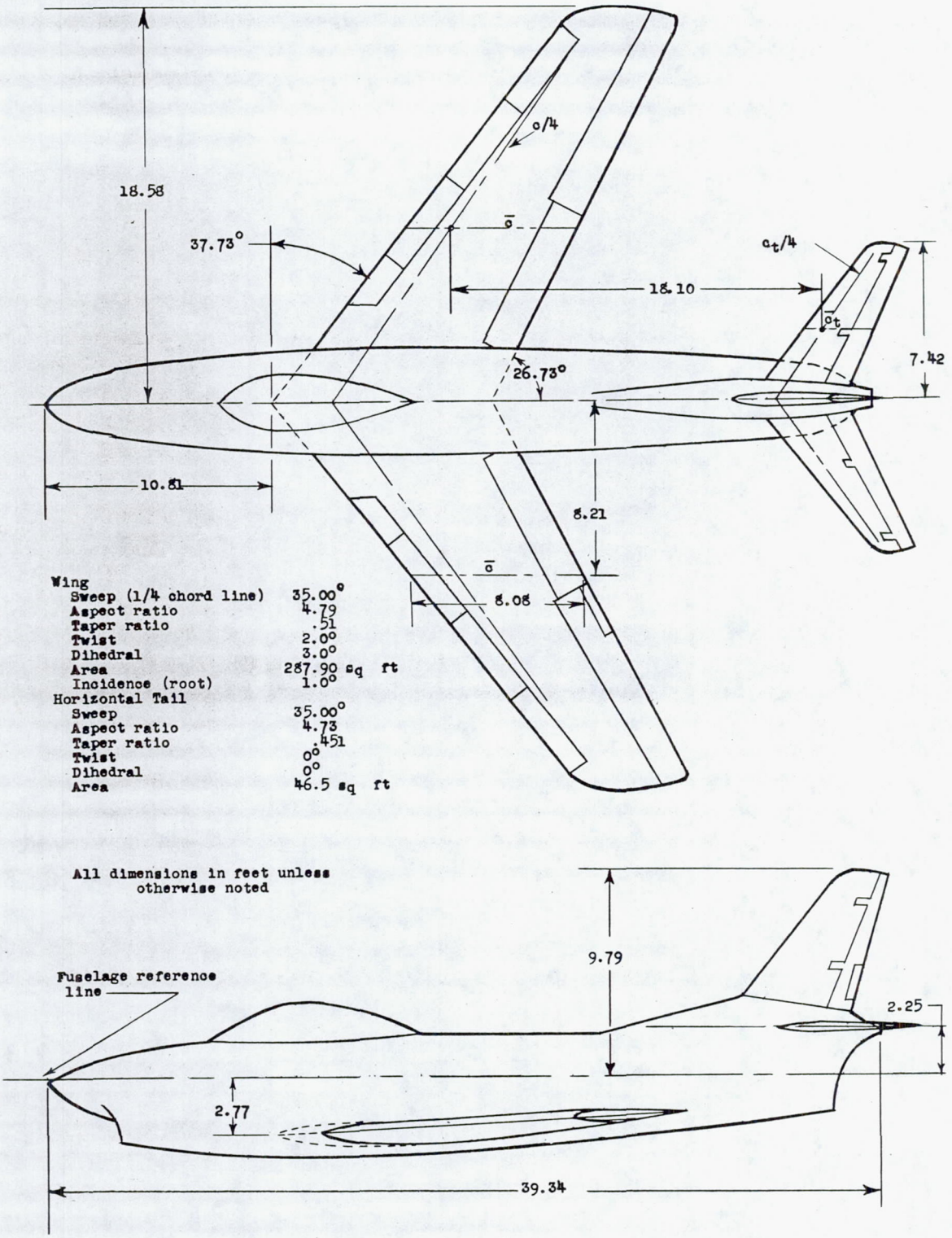
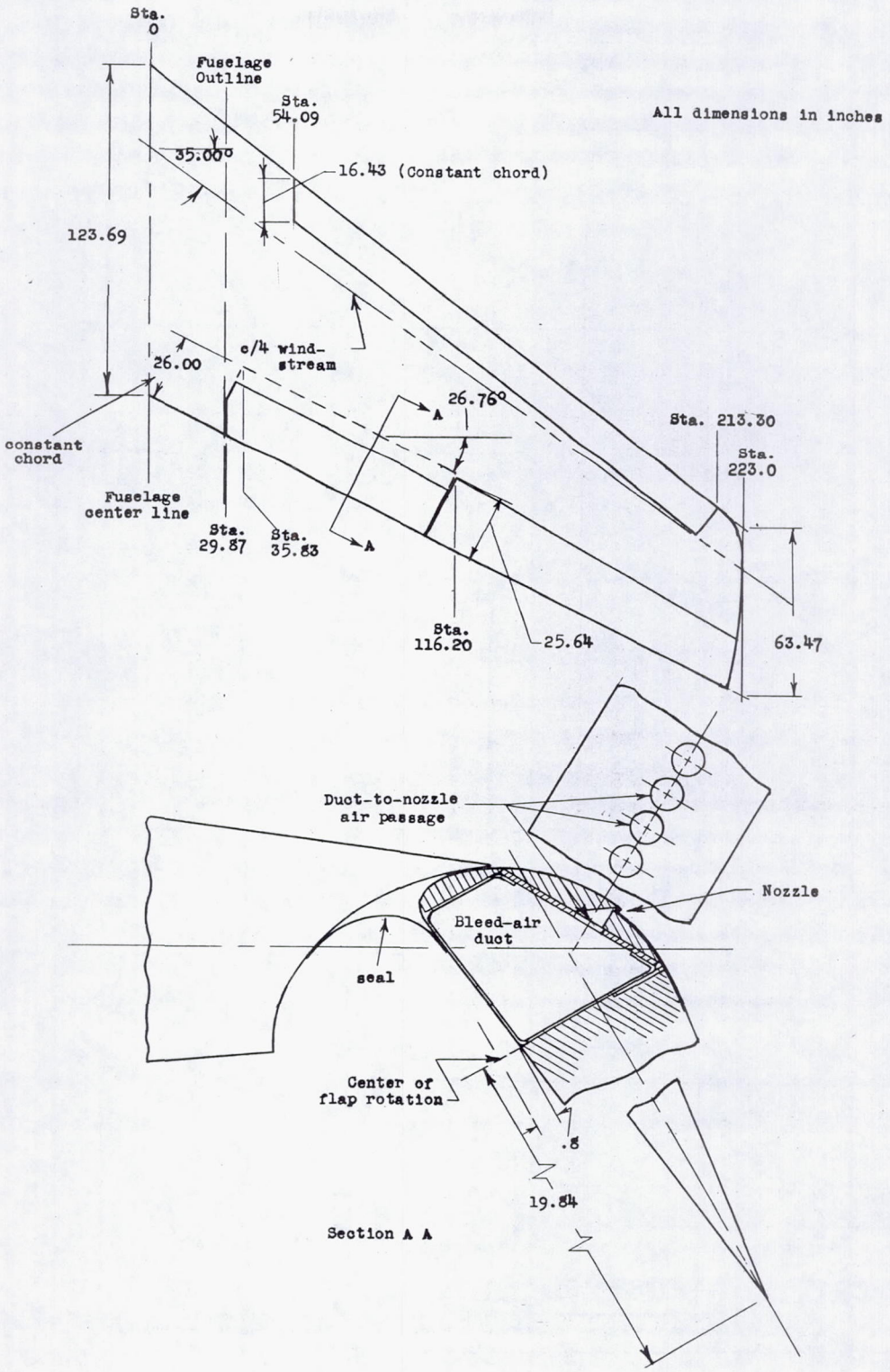
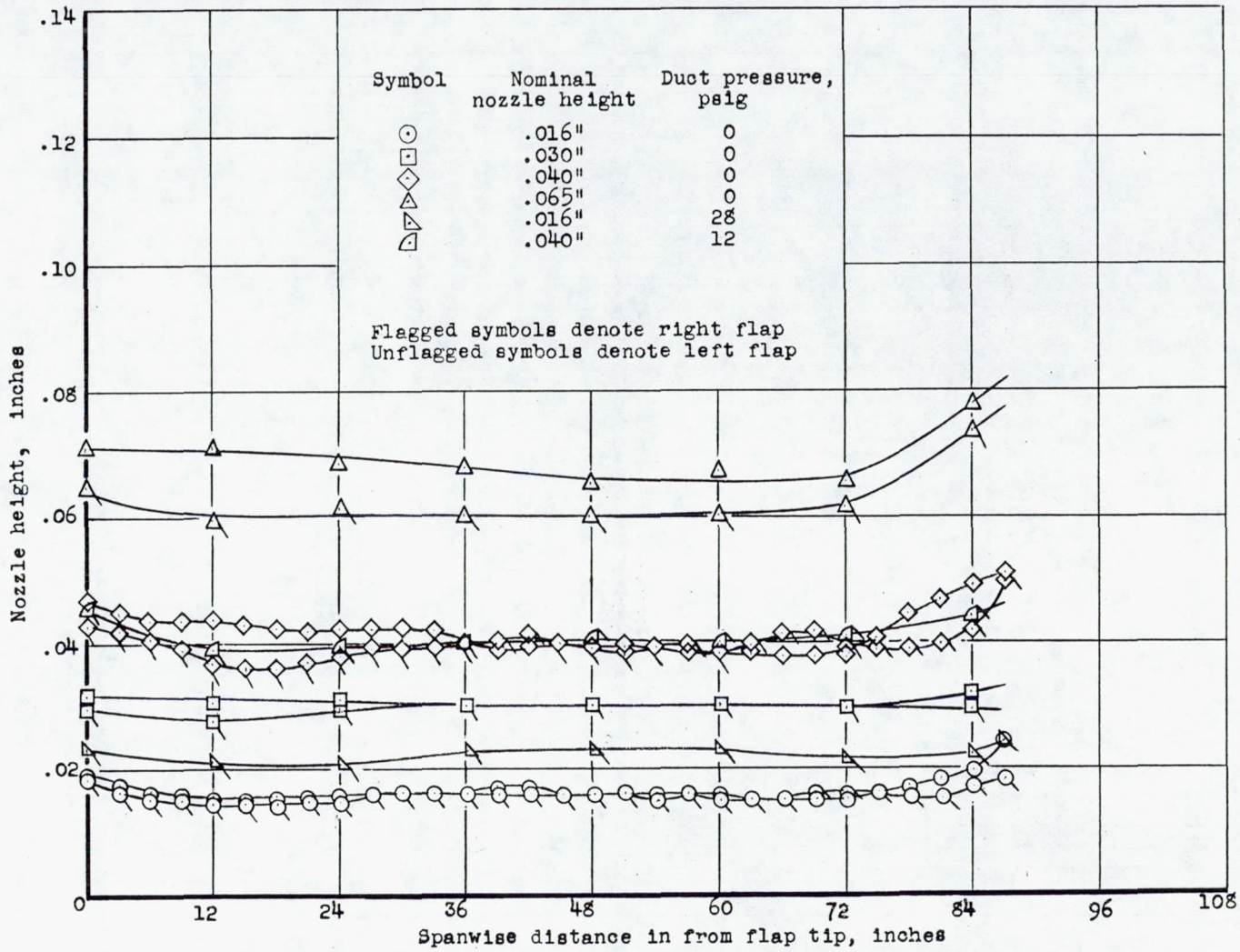


Figure 2.- General arrangement of the YF-86D airplane.



(a) General arrangement.

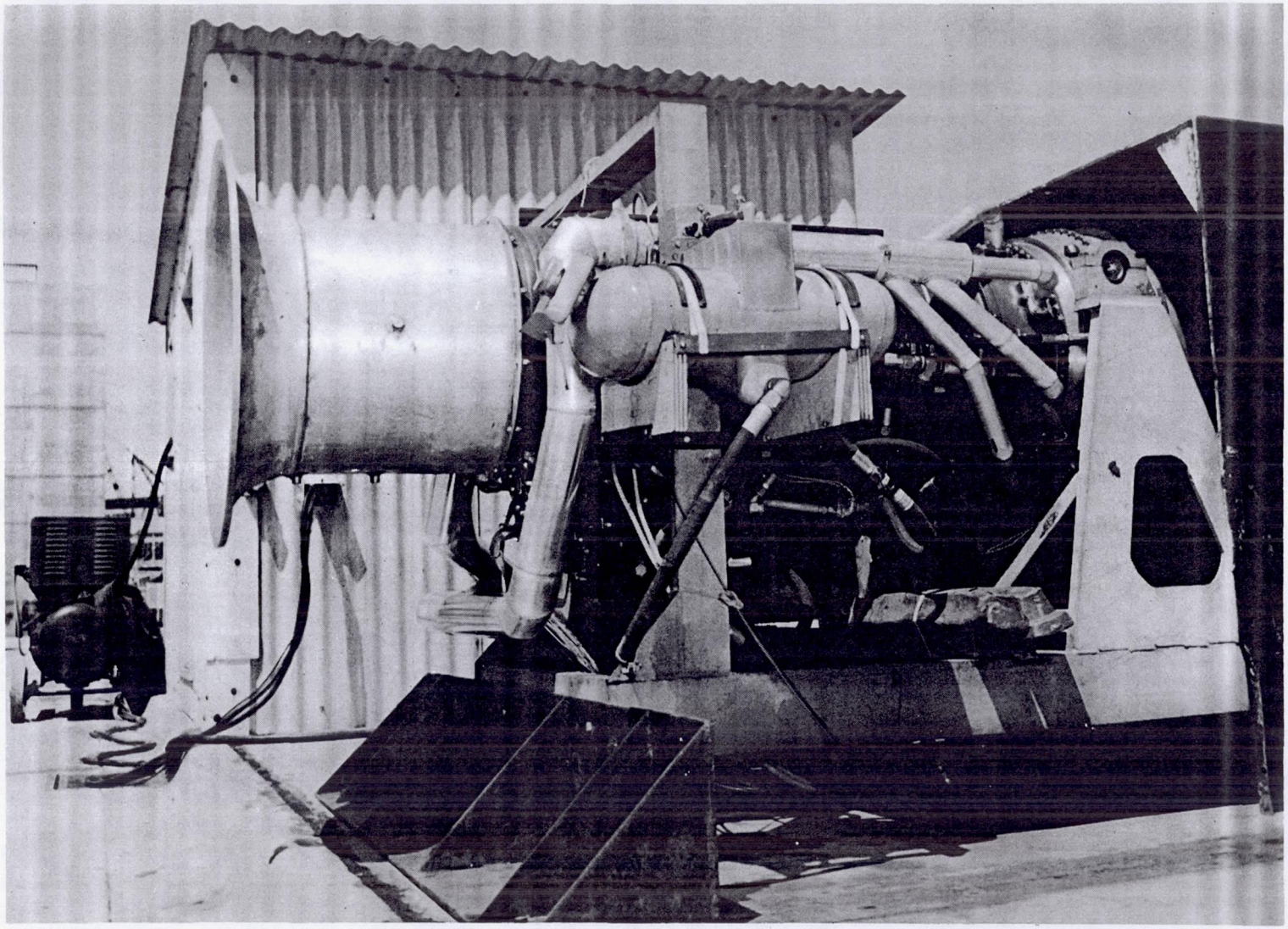
Figure 3.- Details of wing and blowing flap.



(b) Spanwise variation of flap nozzle height.

Figure 3.- Concluded.

CONFIDENTIAL



A-19472

Figure 4.- View of the J-34 engine with bleed-air manifolds installed.

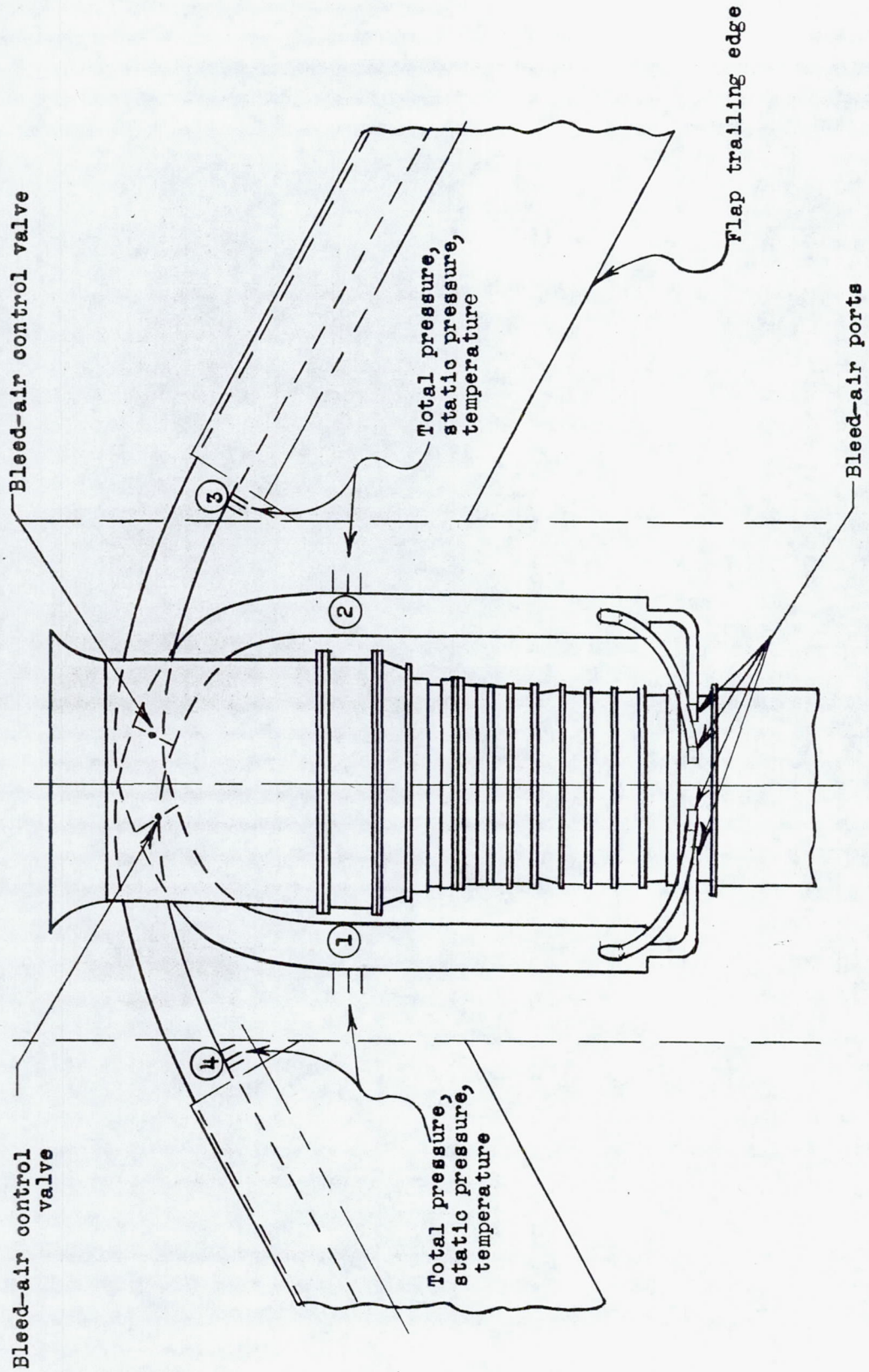
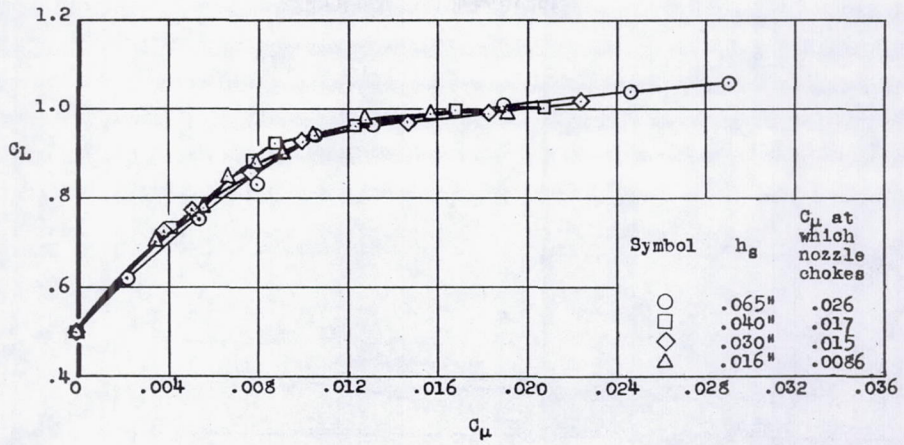
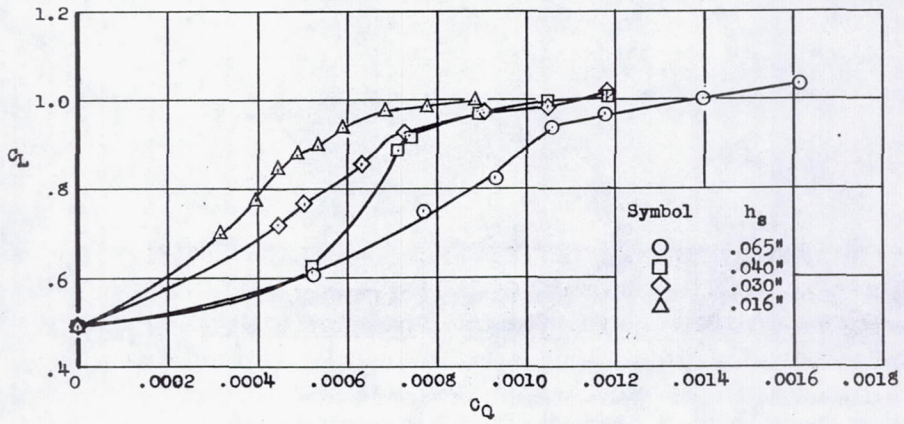


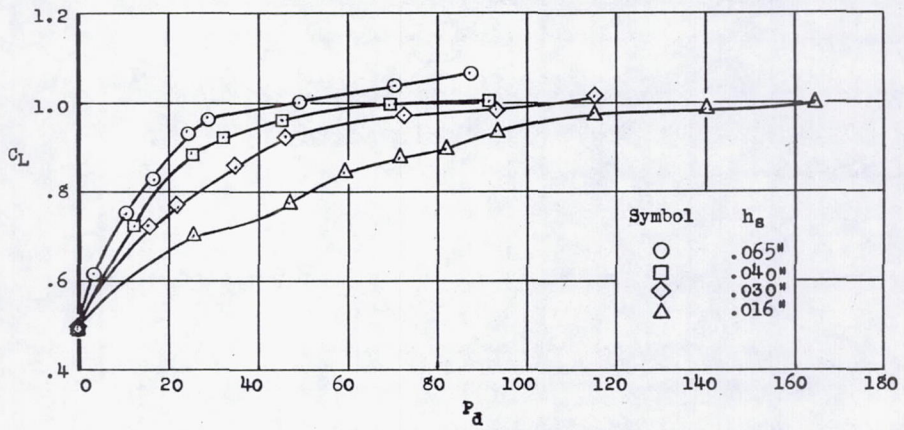
Figure 5.- Sketch of bleed-air ducting.



(a) Variation of lift coefficient with momentum coefficient.

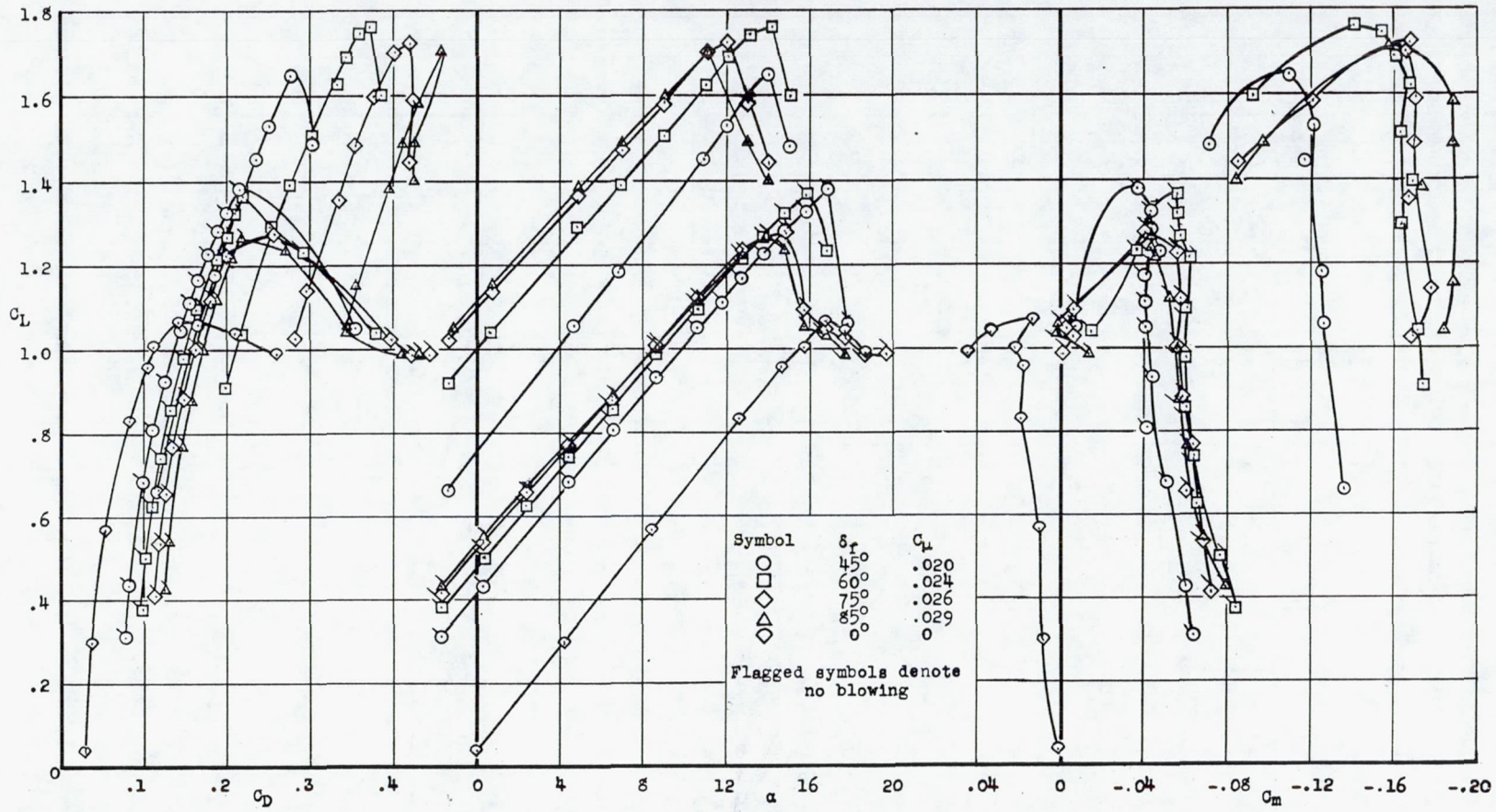


(b) Variation of lift coefficient with flow coefficient.



(c) Variation of lift coefficient with duct pressure coefficient.

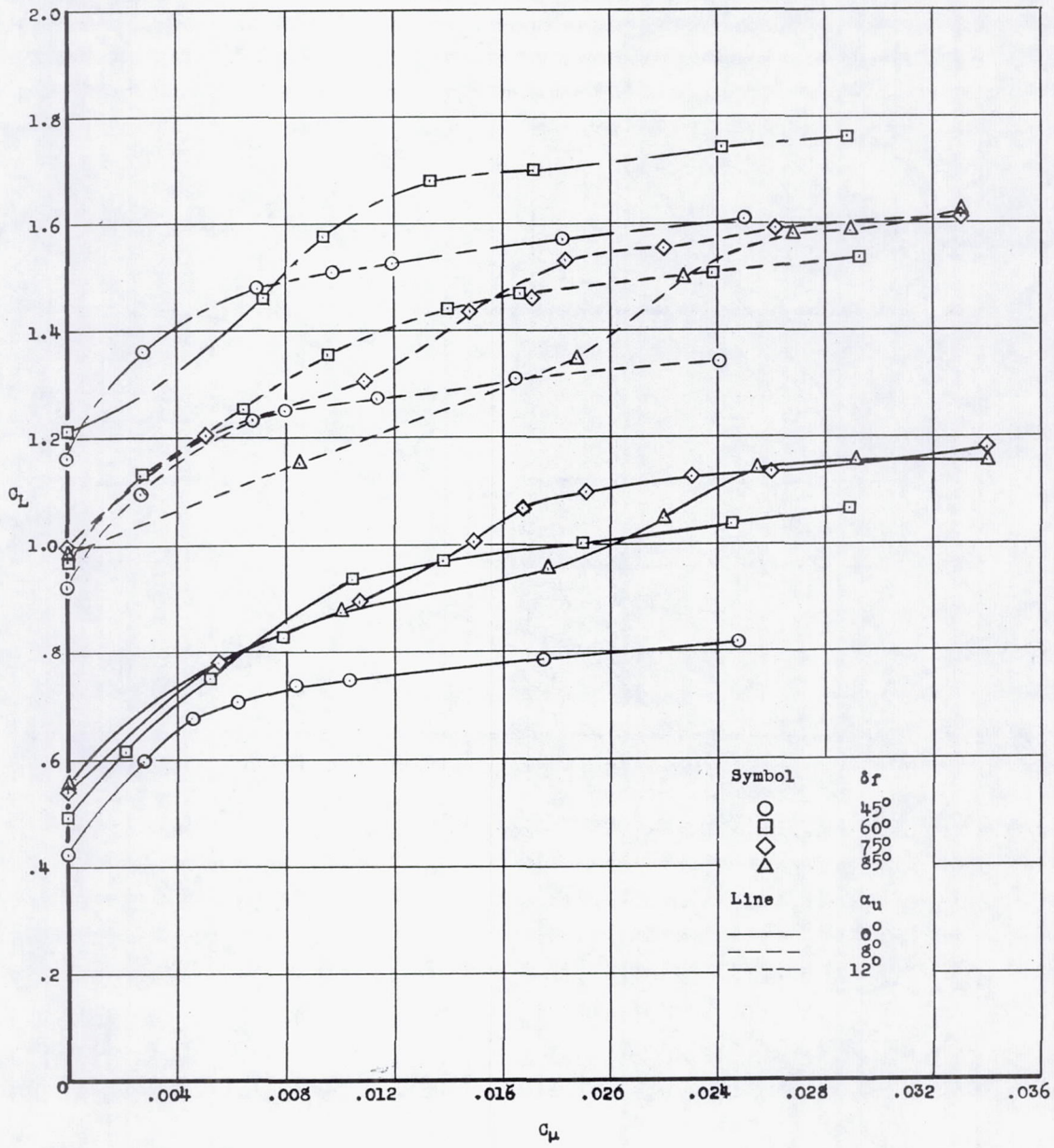
Figure 6.- Effect of nozzle height on the flow requirements of the blowing flap; $\delta_f = 60^\circ$, $\alpha_u = 0^\circ$, R = 7.5×10^6, tail off.



(a) Typical aerodynamic characteristics with and without blowing.

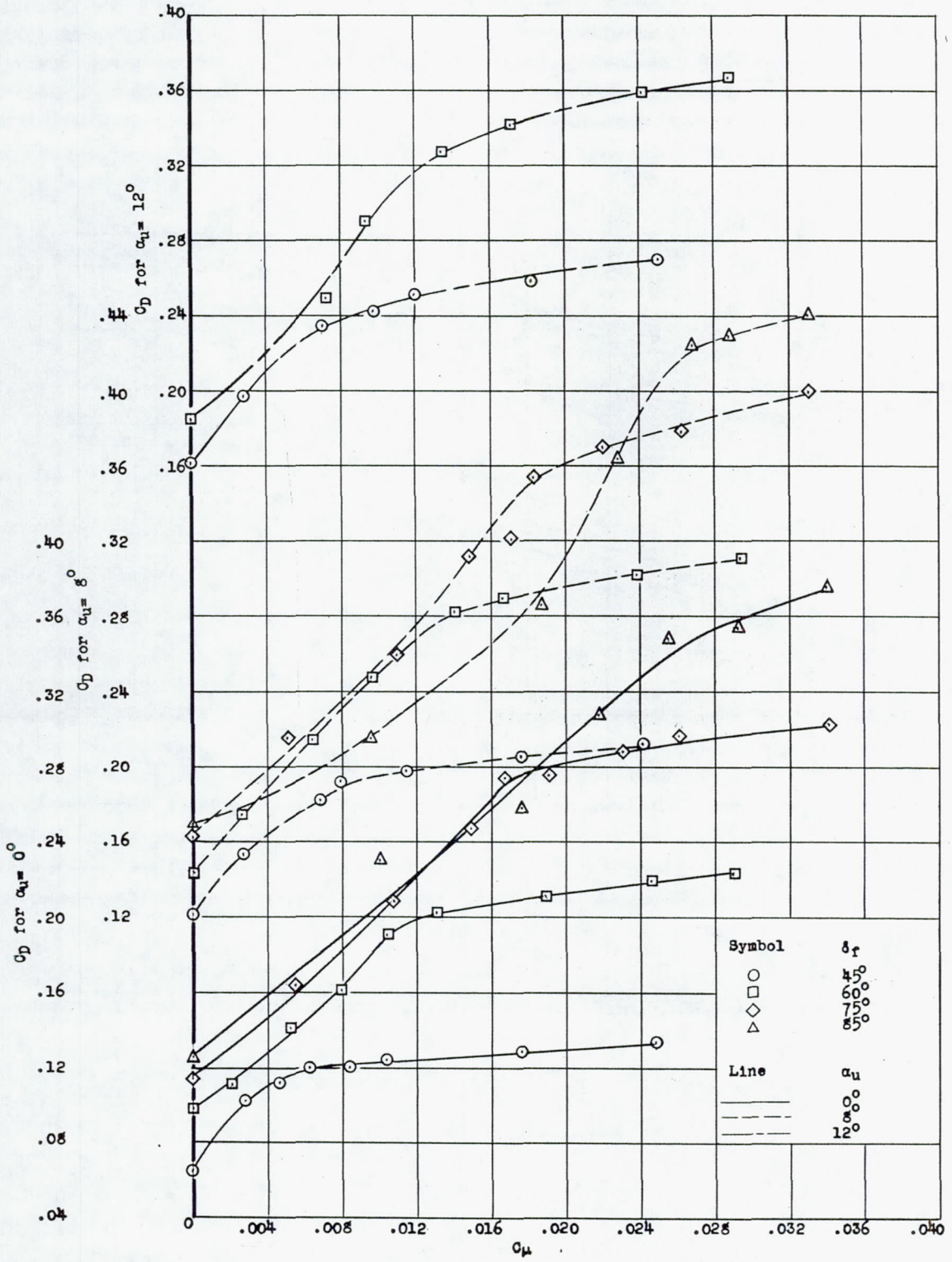
Figure 7.- Effects of blowing over the flaps on the aerodynamic characteristics of the airplane; $R = 7.5 \times 10^6$, tail off, $h_s = 0.065$ inch.

CONFIDENTIAL



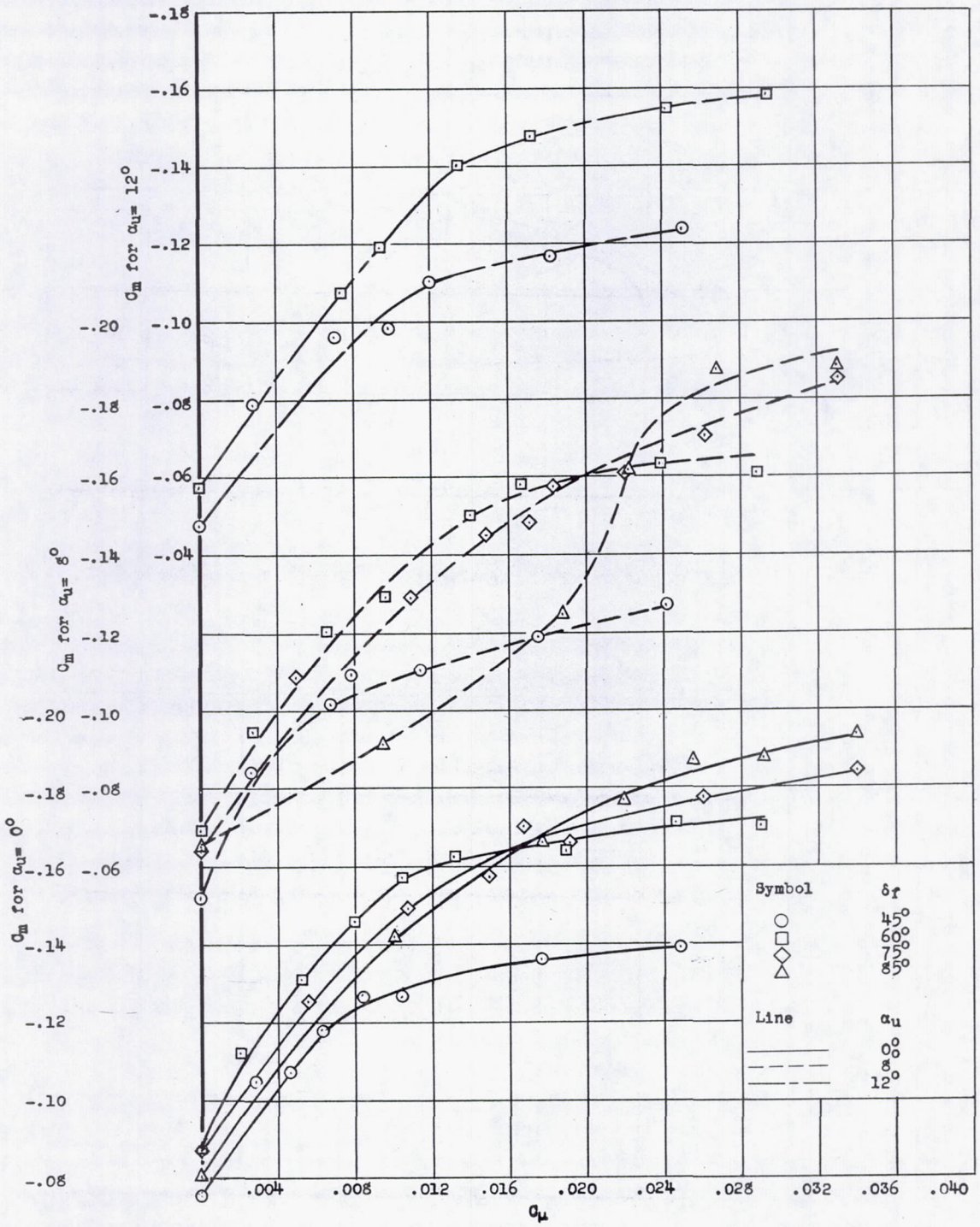
(b) Variation of lift coefficient with momentum coefficient.

Figure 7.- Continued.



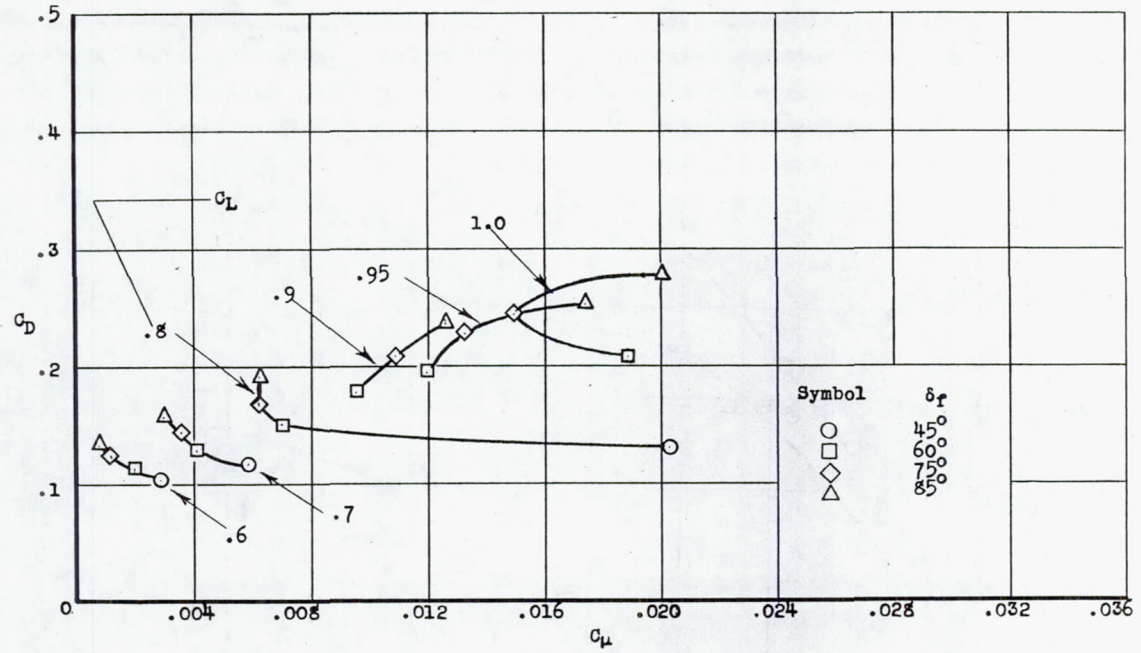
(c) Variation of drag coefficient with momentum coefficient.

Figure 7.- Continued.

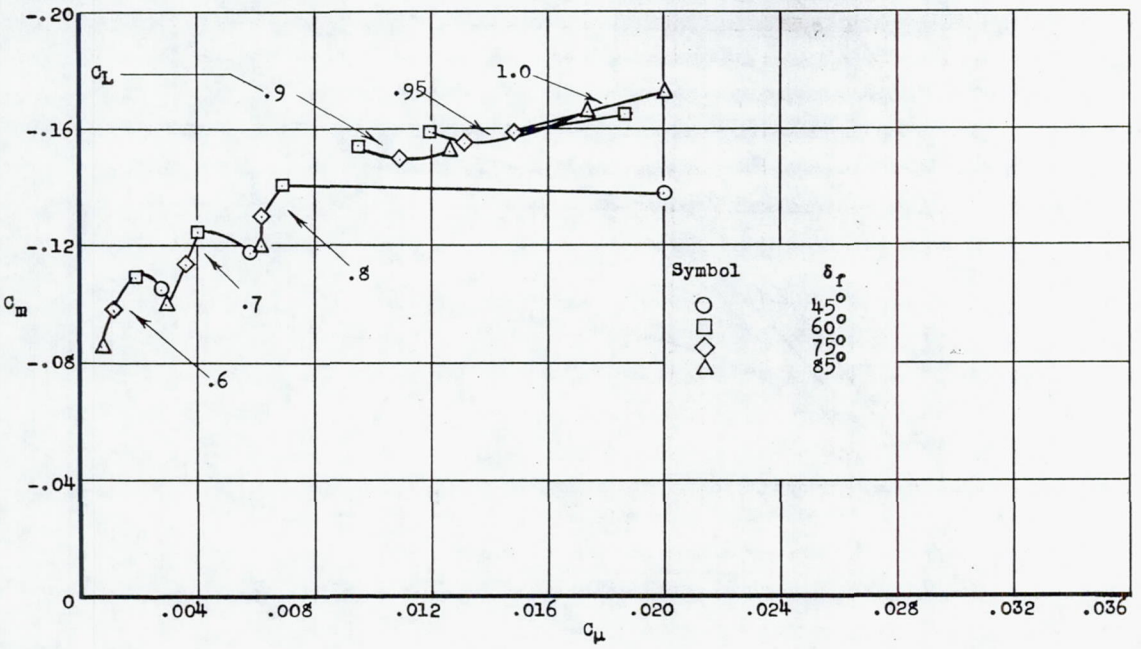


(d) Variation of pitching-moment coefficient with momentum coefficient.

Figure 7.- Concluded.



(a) Variation of drag coefficient with momentum coefficient.



(b) Variation of pitching-moment coefficient with momentum coefficient.

Figure 8.- Effects of blowing over the flaps on the aerodynamic characteristics of the airplane at various lift coefficients; R = 7.5×10^6, tail off, h_s = 0.065 inch, α_u = 0°.

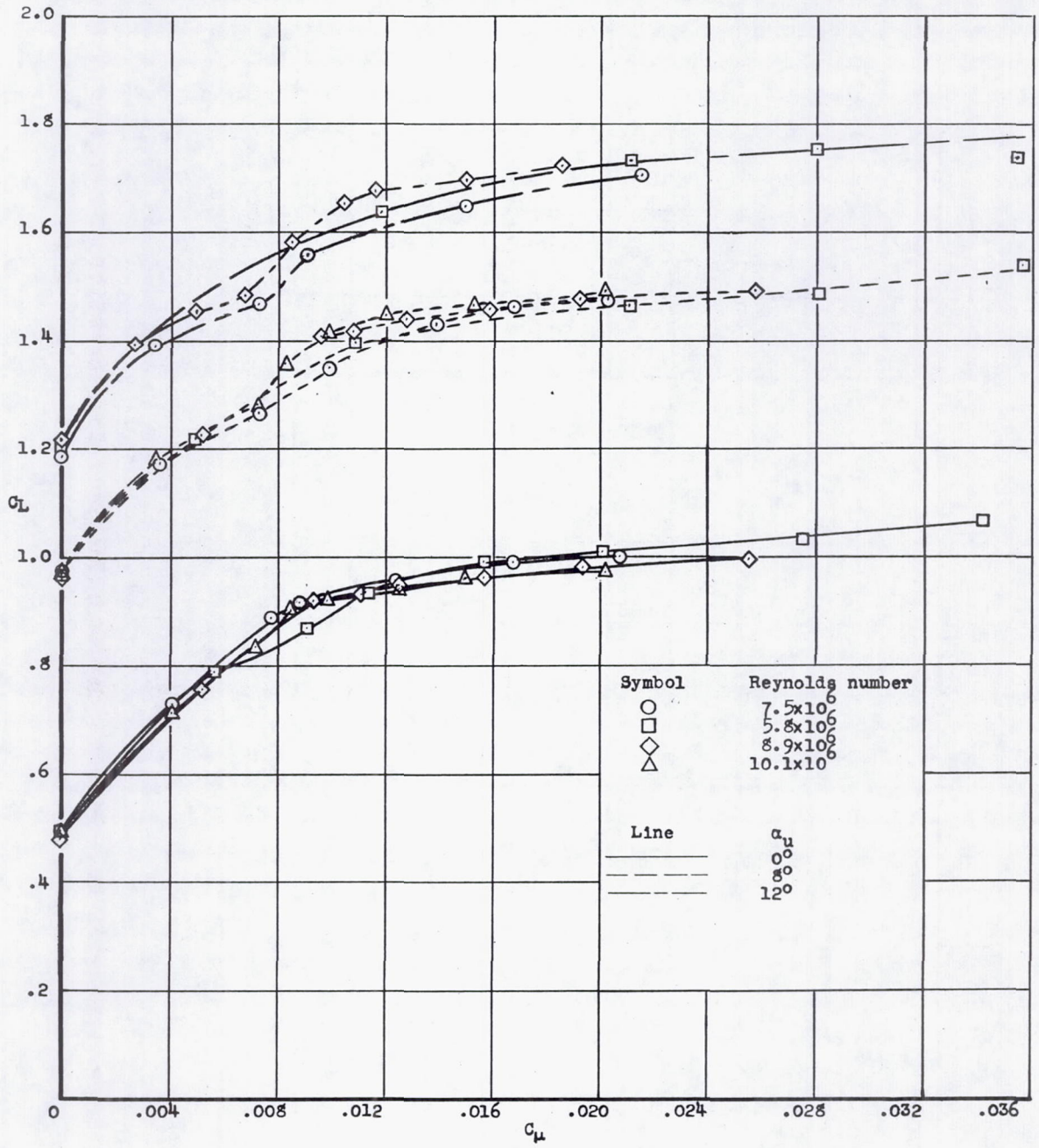
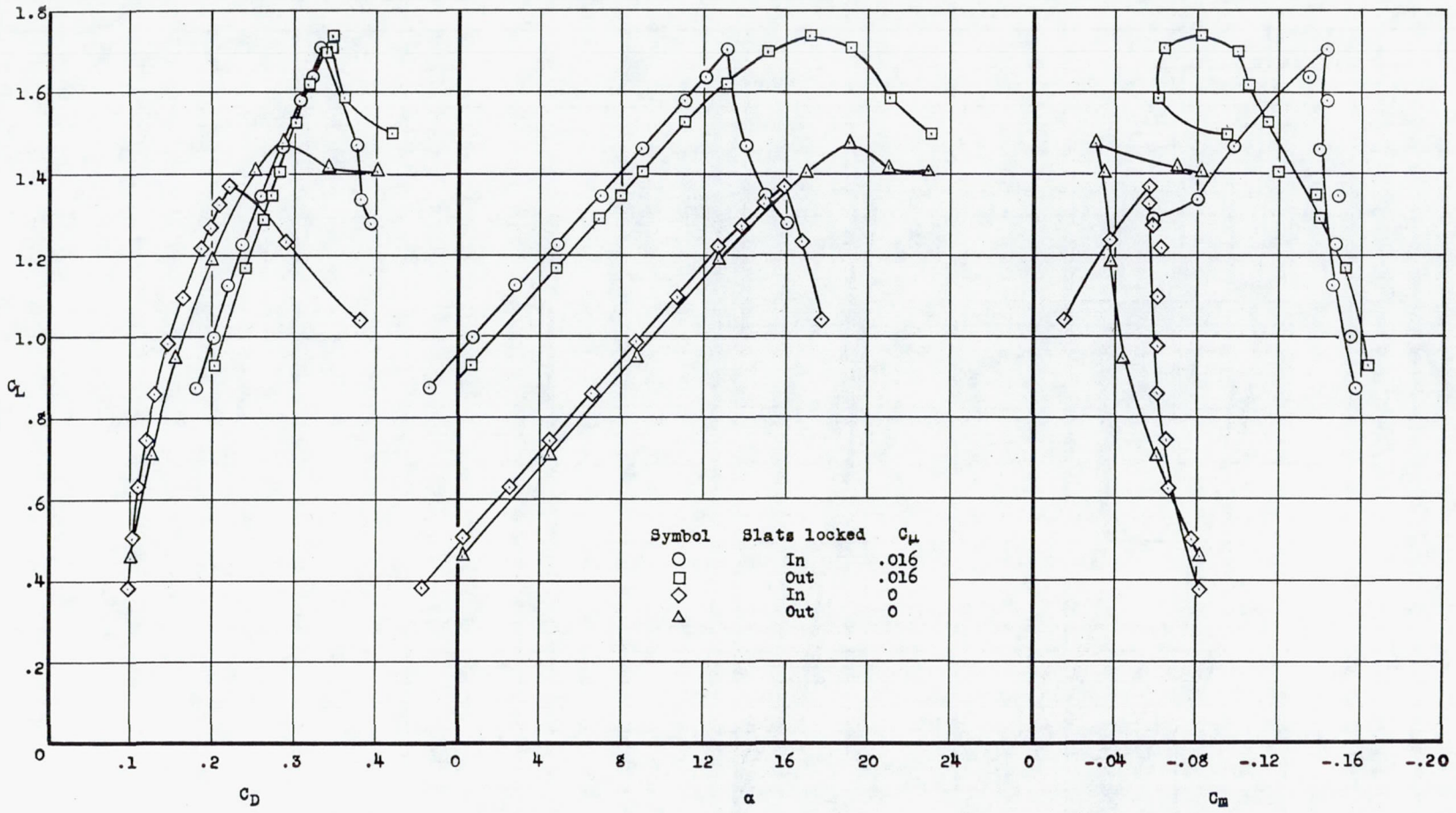


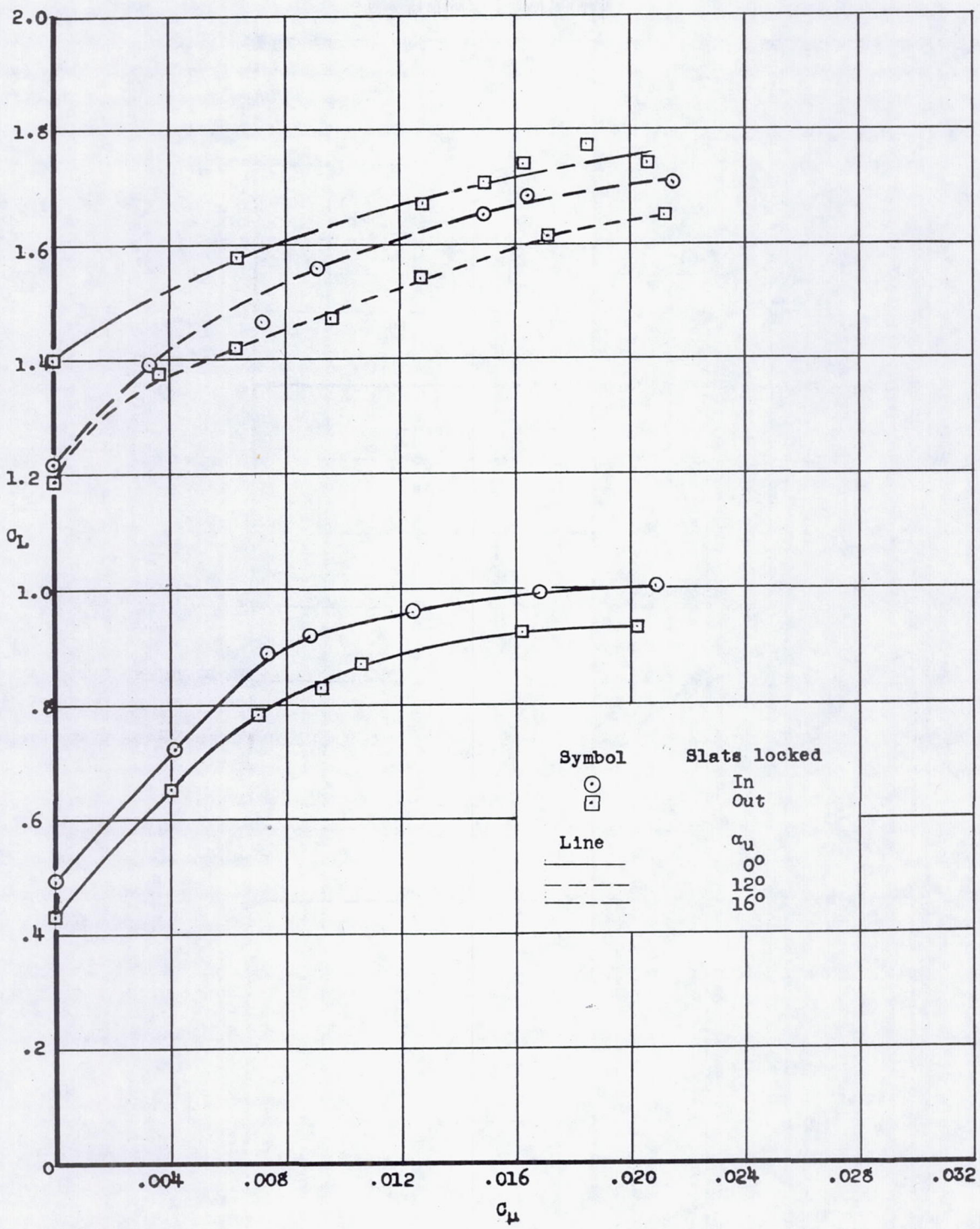
Figure 9.- Variation of lift coefficient with momentum coefficient for various Reynolds numbers; $\delta_f = 60^\circ$, tail off, $h_s = 0.040$ inch.



(a) Typical aerodynamic characteristics with and without leading-edge slats.

Figure 10.- Effects of leading-edge slats on the aerodynamic characteristics of the airplane with blowing over the flaps; $\delta_f = 60^\circ$, $R = 7.5 \times 10^6$, tail off, $h_s = 0.040$ inch.

CONFIDENTIAL



(b) Variation of lift coefficient with momentum coefficient.

Figure 10.- Concluded.

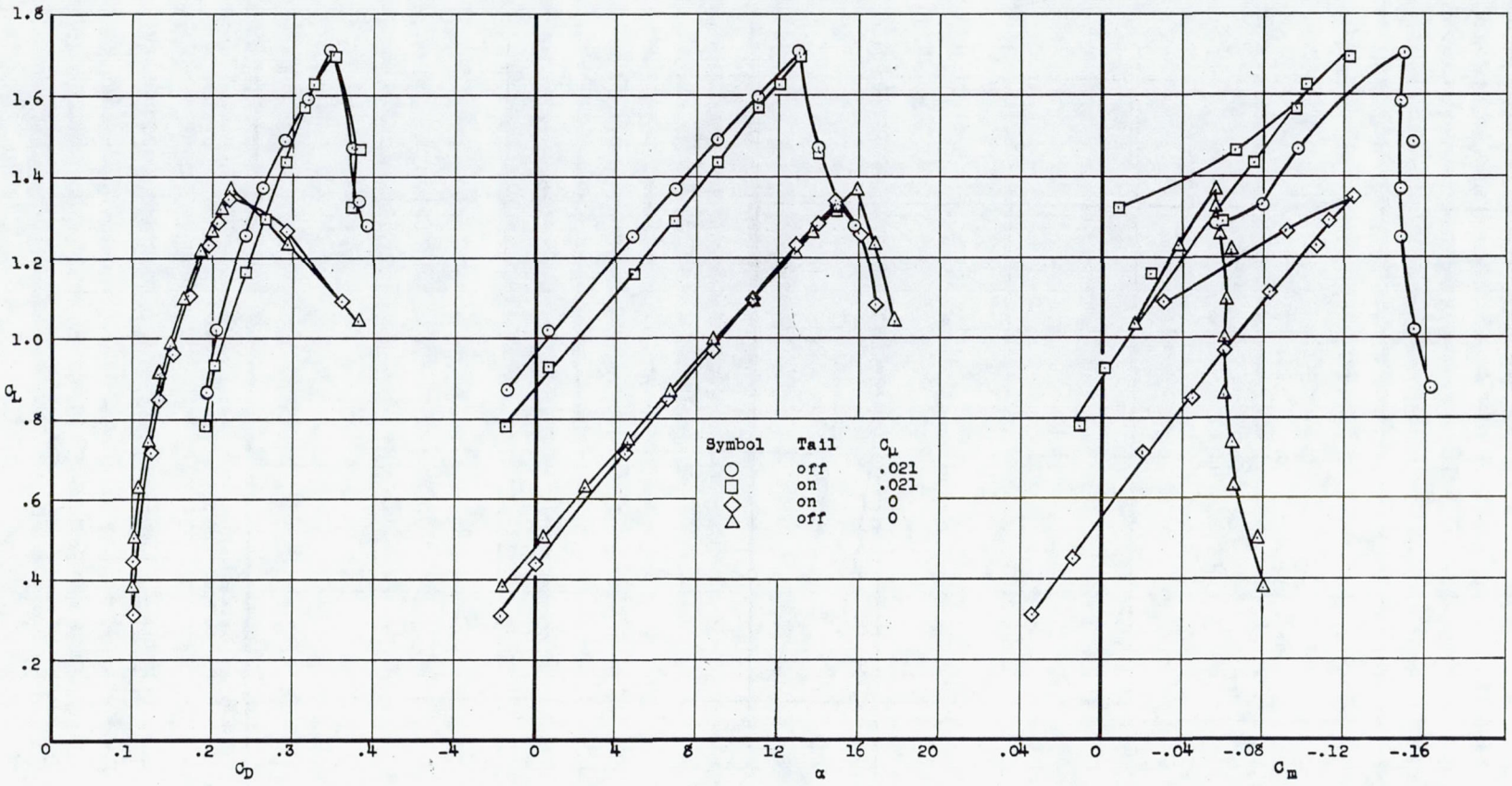
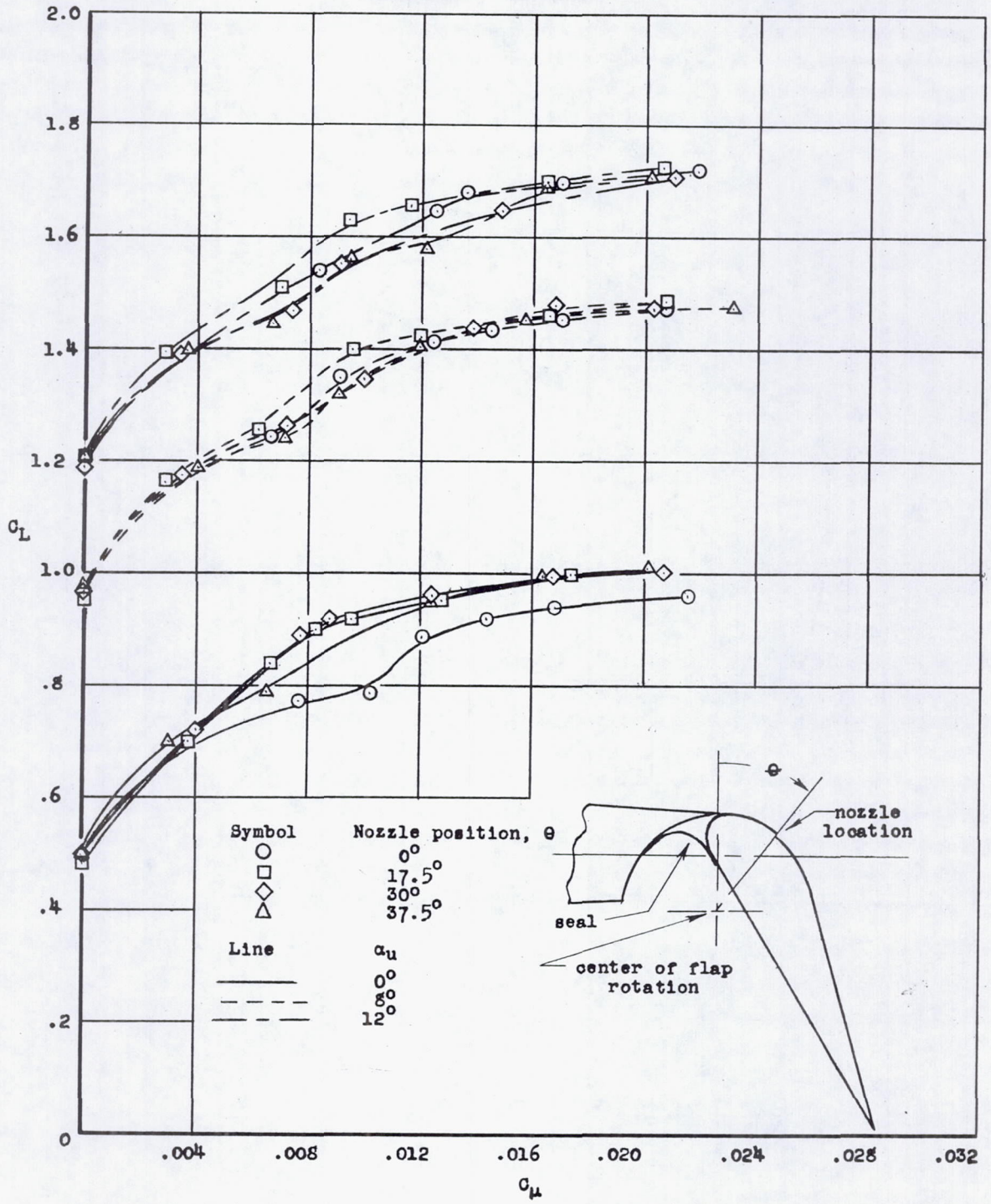
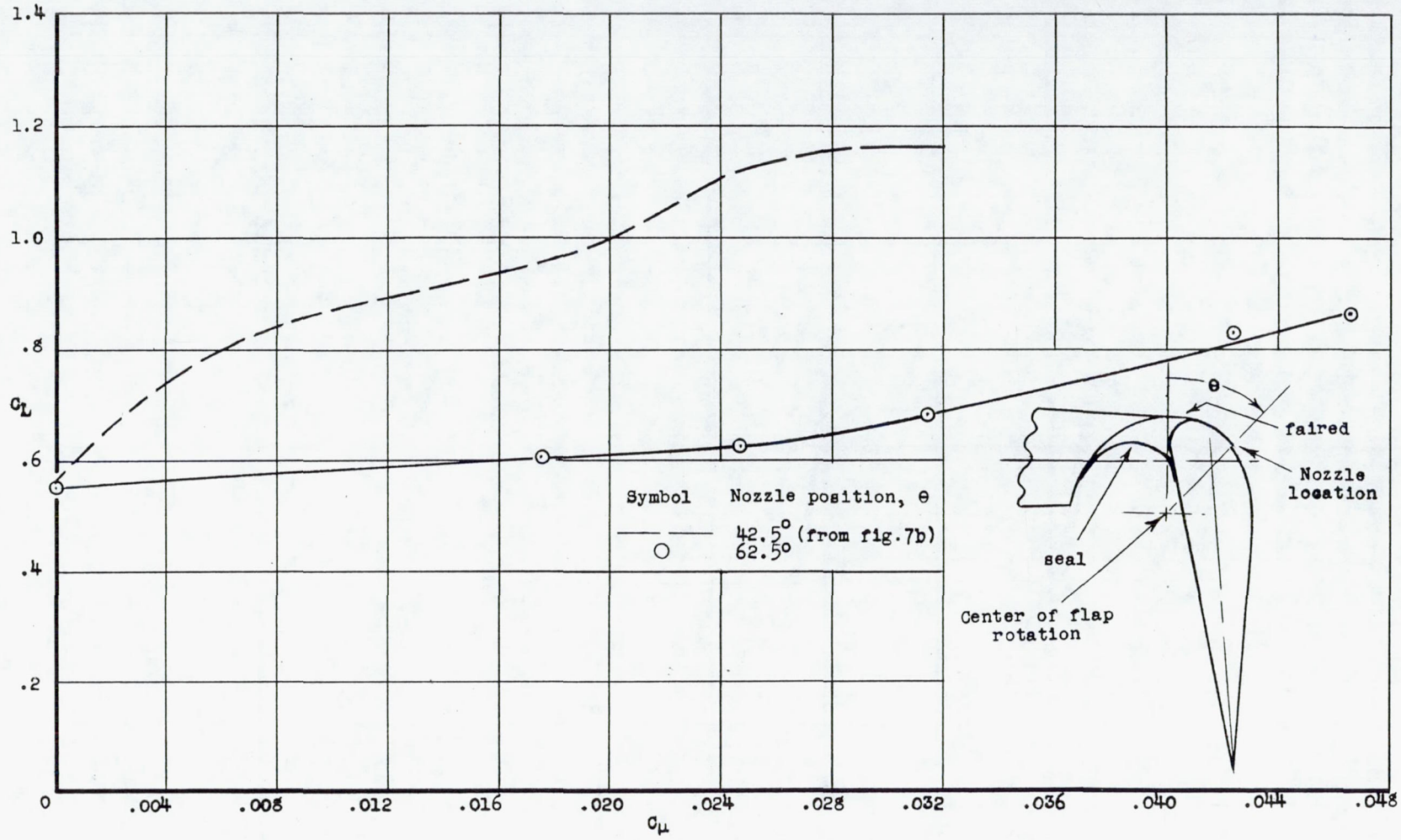


Figure 11.- Aerodynamic characteristics of the airplane with and without the horizontal tail; $\delta_f = 60^\circ$, $R = 7.5 \times 10^6$, $h_s = 0.040$ inch, tail incidence = 0°.



(a) $\delta_f = 60^\circ$, $h_s = 0.040$ inch

Figure 12.- Variation of lift coefficient with momentum coefficient for various nozzle locations; $\delta_f = 60^\circ$, $R = 7.5 \times 10^6$, tail off.



(b) $\delta_f = 85^\circ$, $h_s = 0.065$ inch

Figure 12.- Concluded.

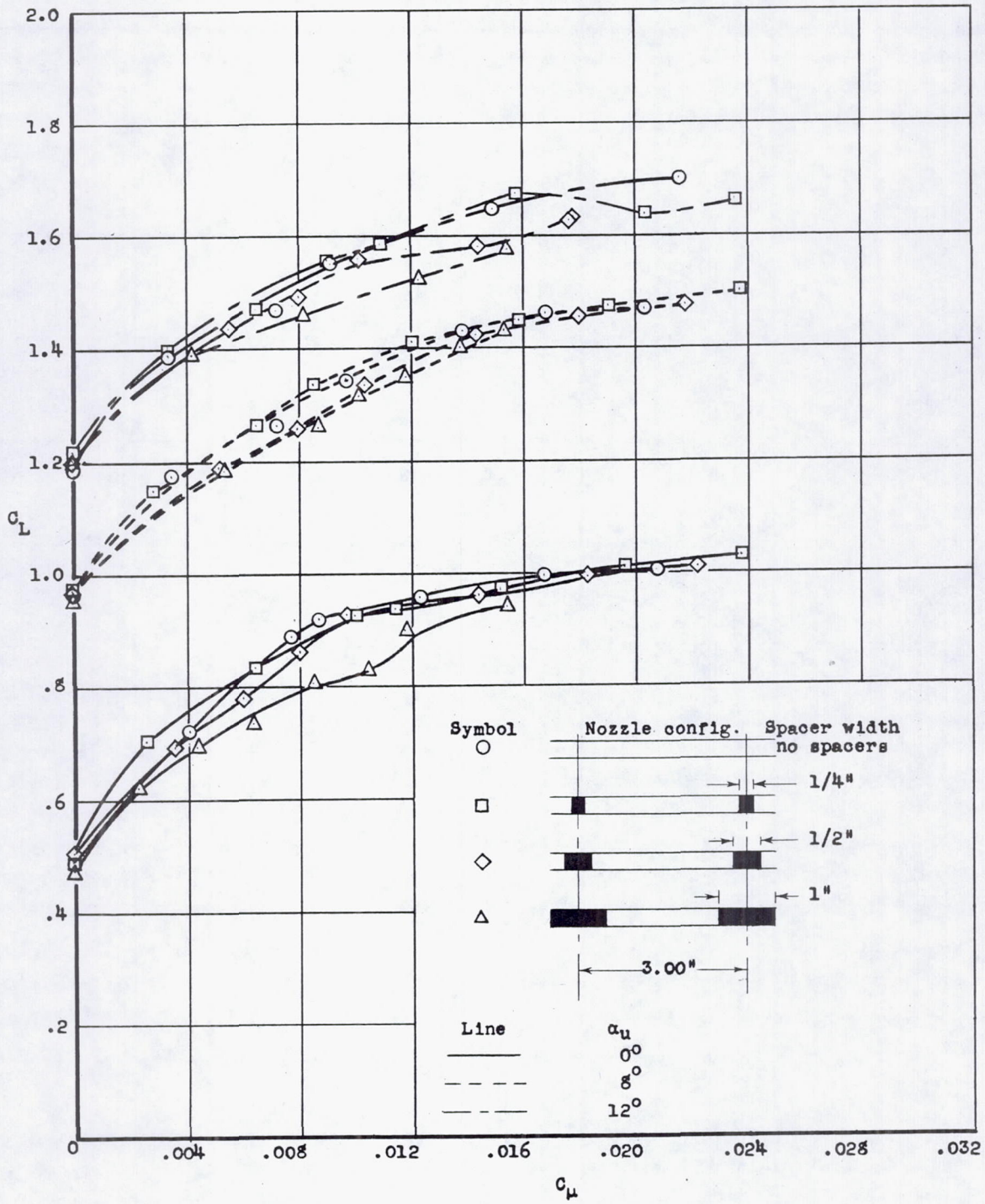


Figure 13.- Variation of lift coefficient with momentum coefficient for nozzles having various spacer arrangements; $\delta_f = 60^\circ$, $R = 7.5 \times 10^6$, tail off, $h_s = 0.040$ inch.

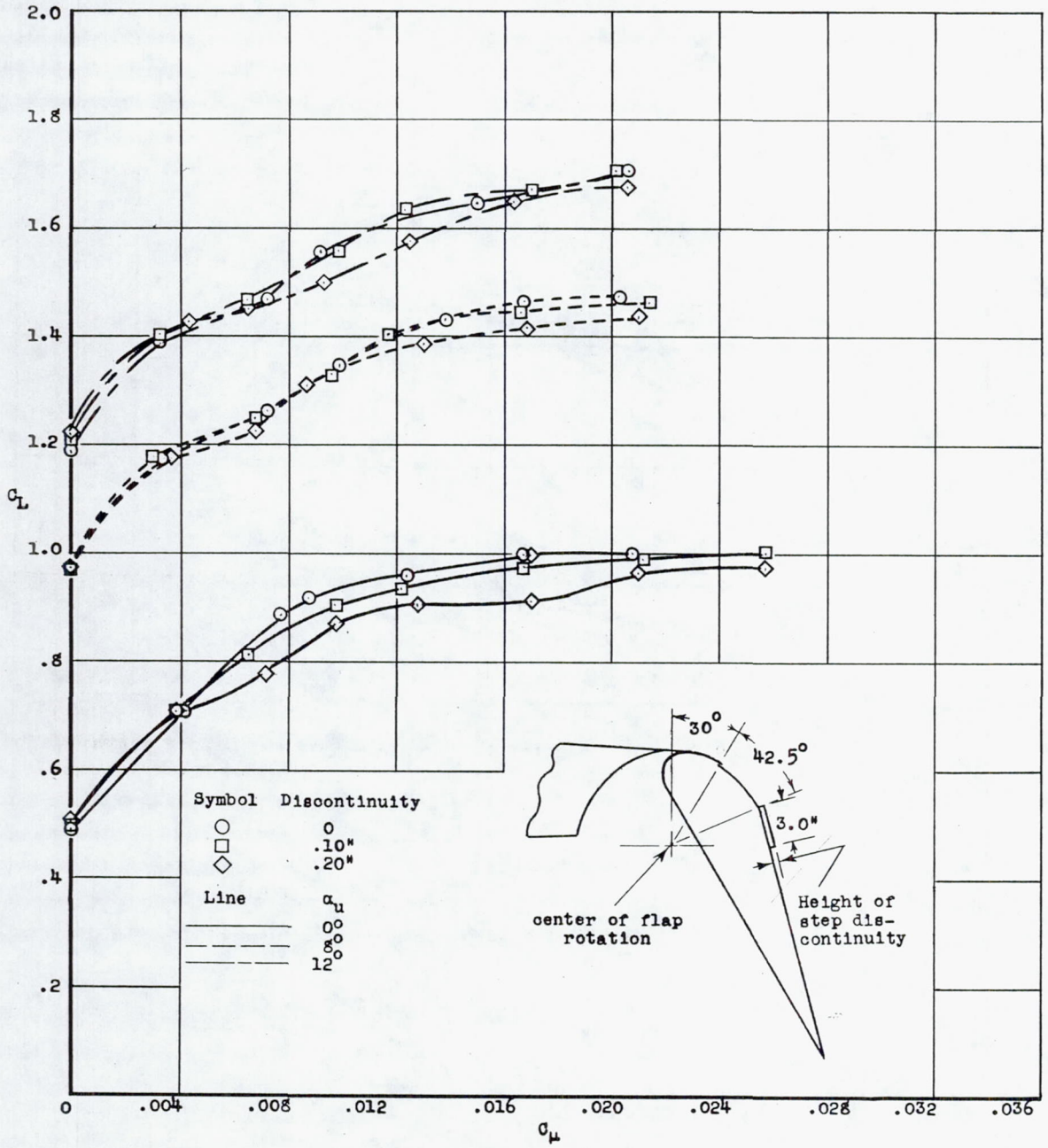


Figure 14.- Variation of lift coefficient with momentum coefficient for various discontinuities on the flap surface; $\delta_f = 60^\circ$, $R = 7.5 \times 10^6$, tail off, $h_s = 0.040$ inch.

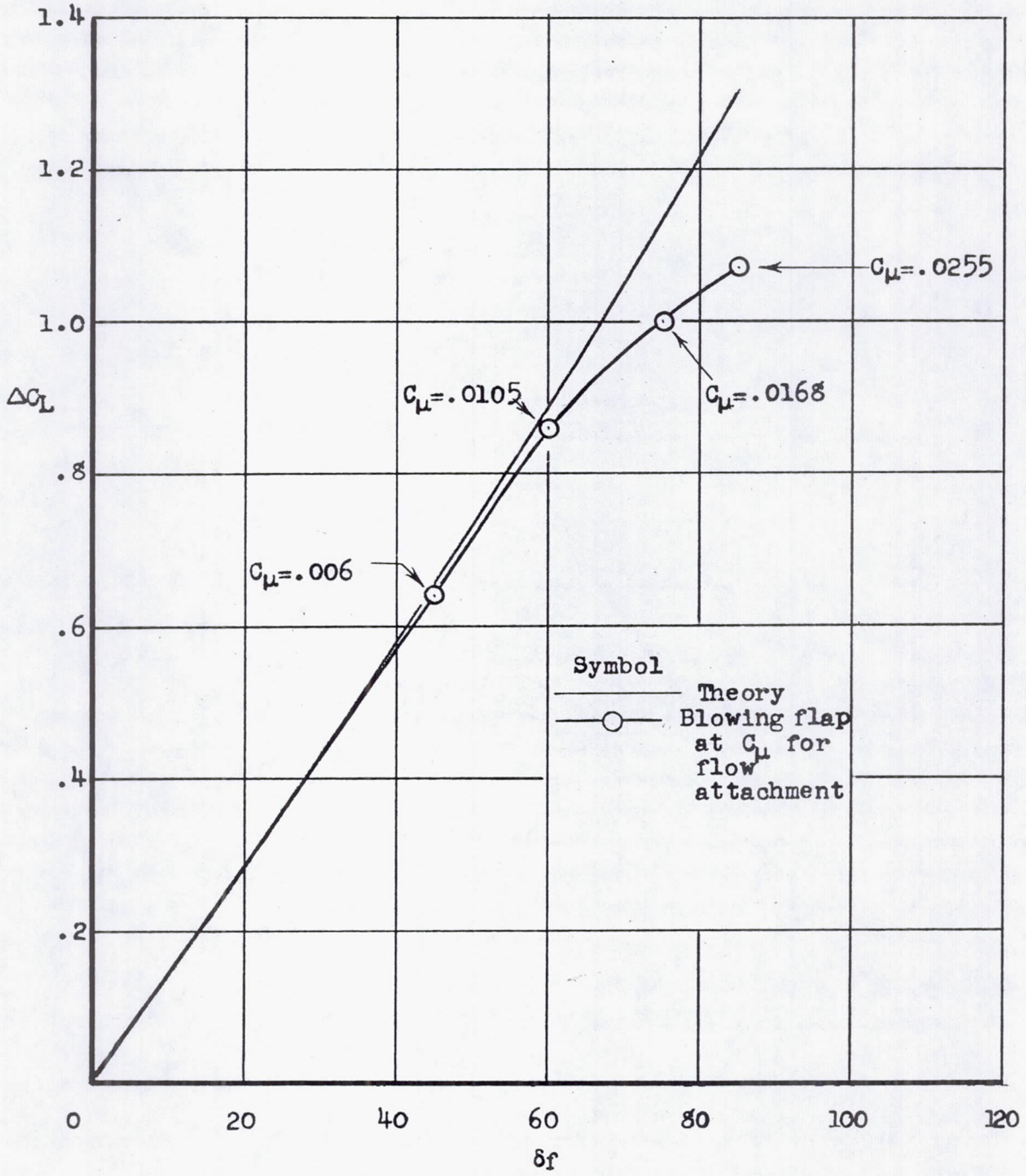
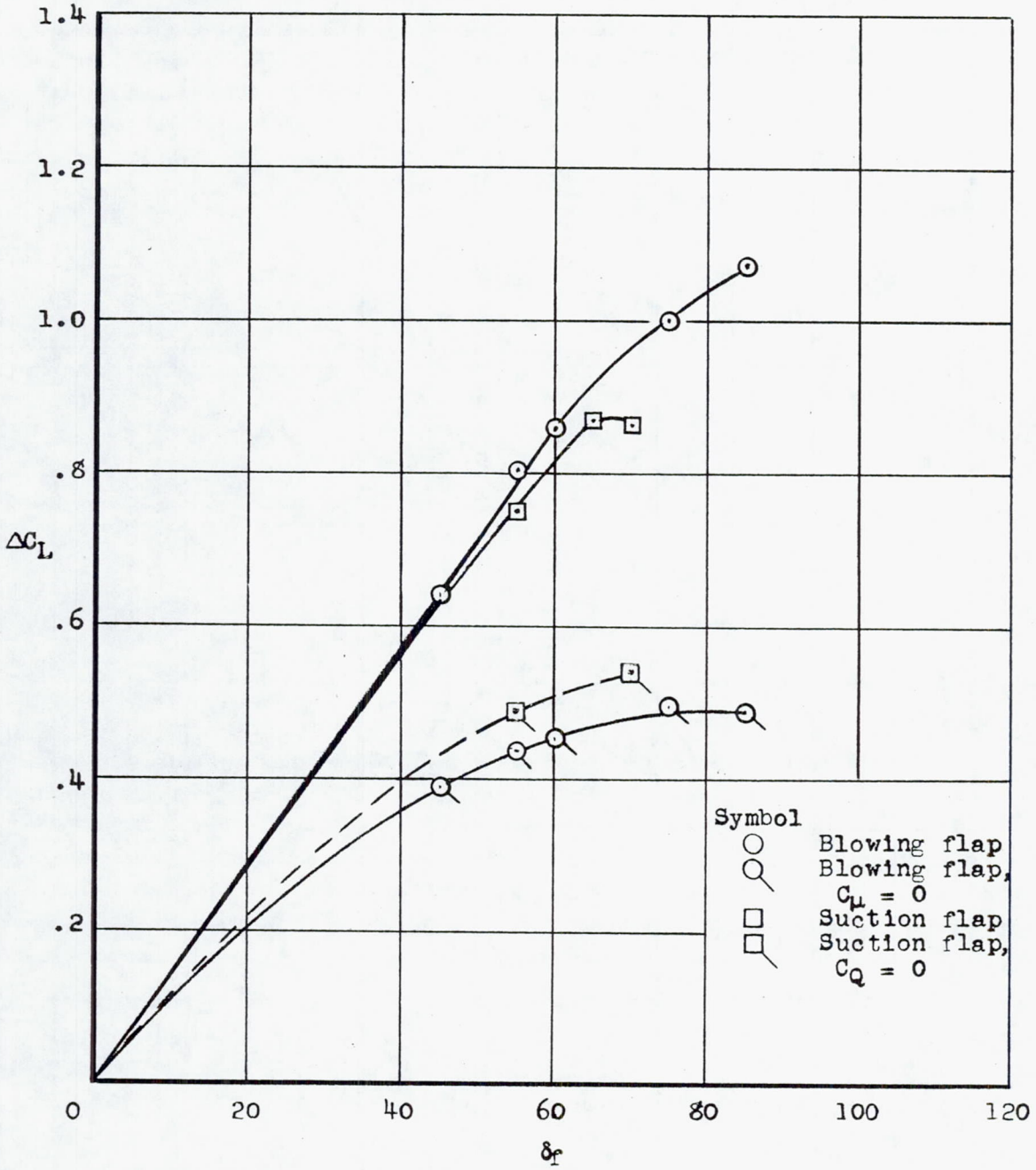
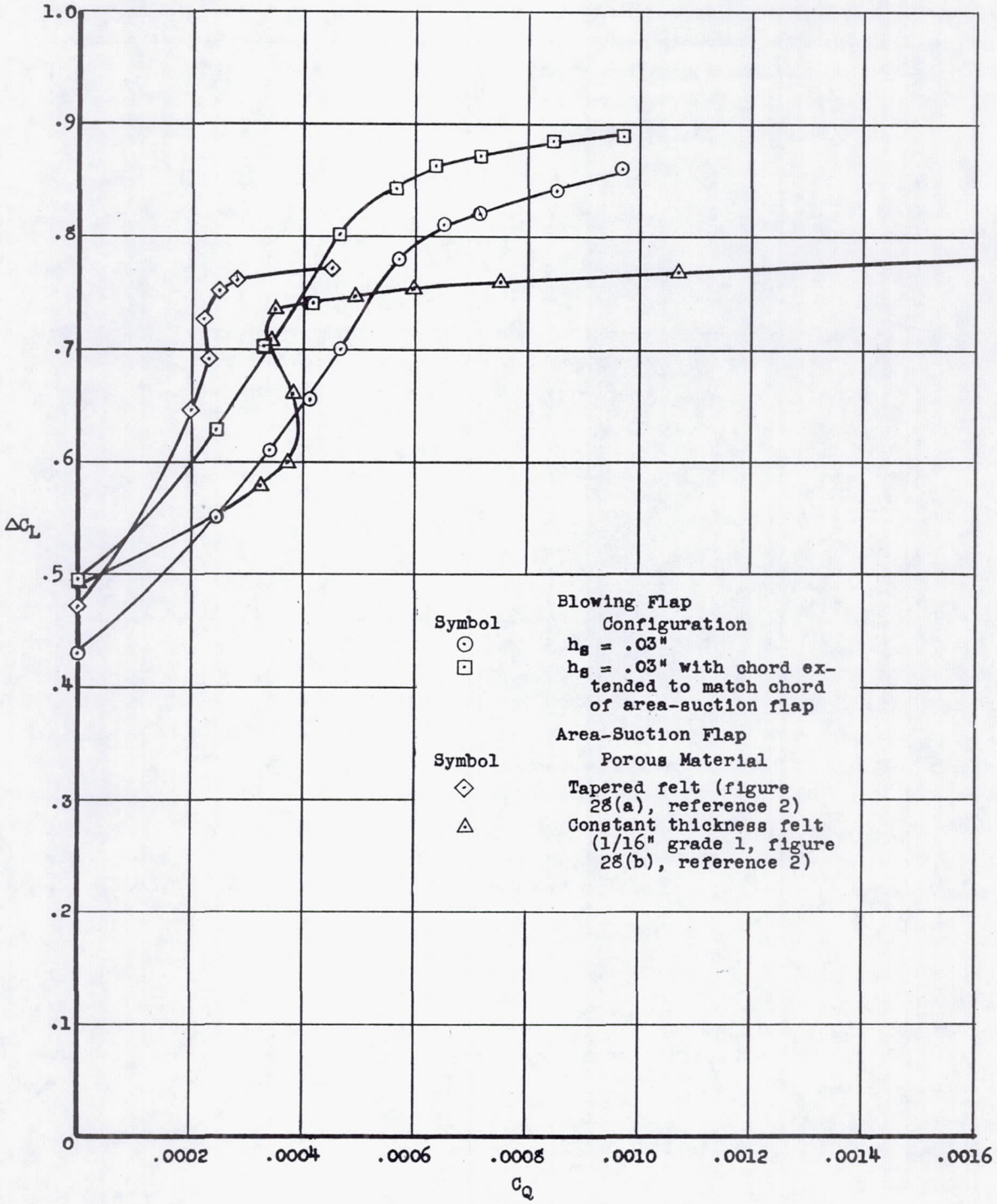


Figure 15.- Comparison of theoretical flap lift increments with those obtained experimentally on the blowing flap at the point of flow attachment; $\alpha = 0^\circ$.



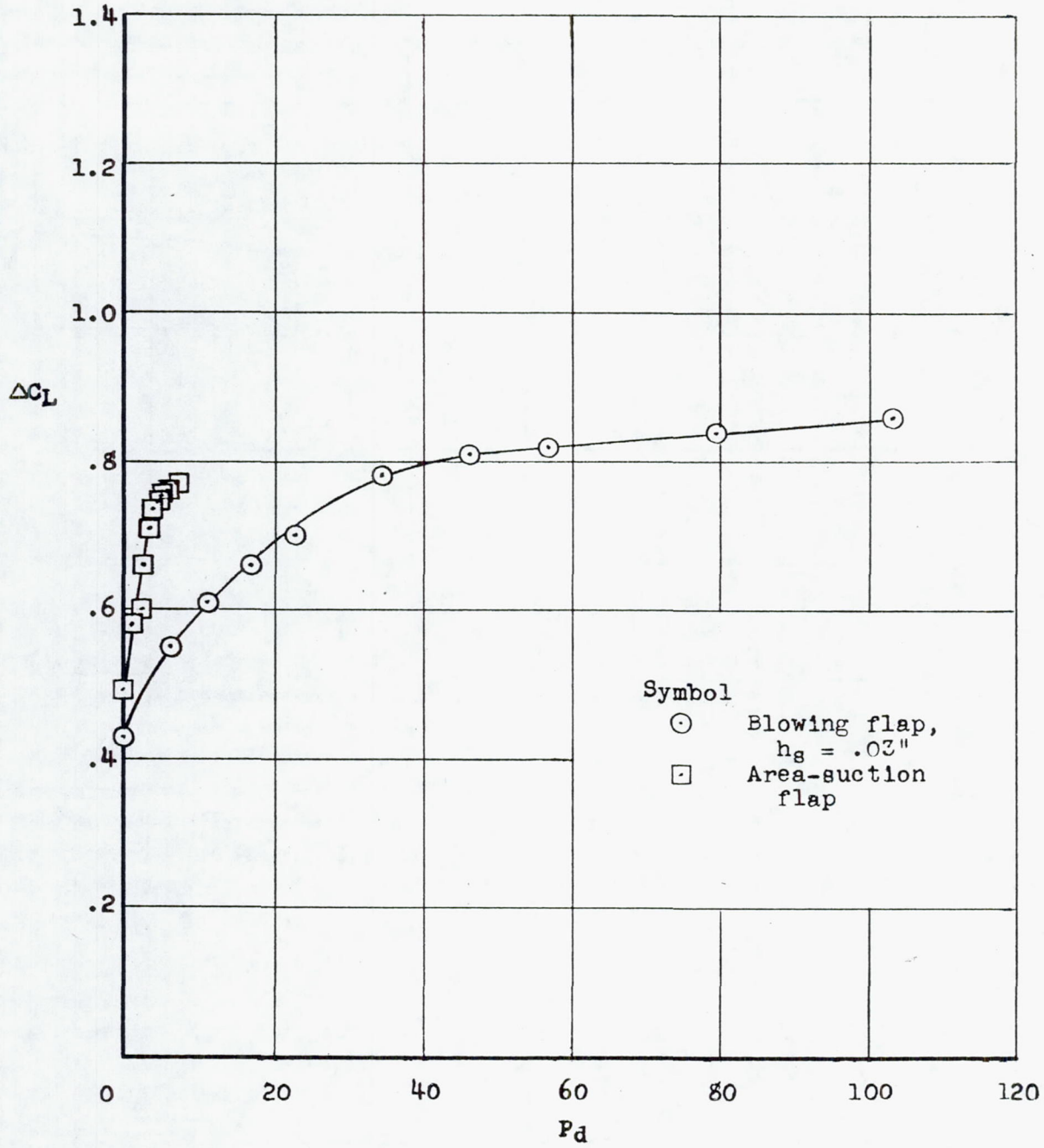
(a) Variation of lift-coefficient increment with flap deflection.

Figure 16.- Comparison of area-suction and blowing flaps; $\alpha = 0^\circ$, $R = 7.5 \times 10^6$, tail off.



(b) Variation of lift-coefficient increment with flow coefficient; $\delta_f = 55^\circ$.

Figure 16.- Continued.



(c) Variation of lift-coefficient increment with duct pressure coefficient; $\delta_f = 55^\circ$.

Figure 16.- Concluded.

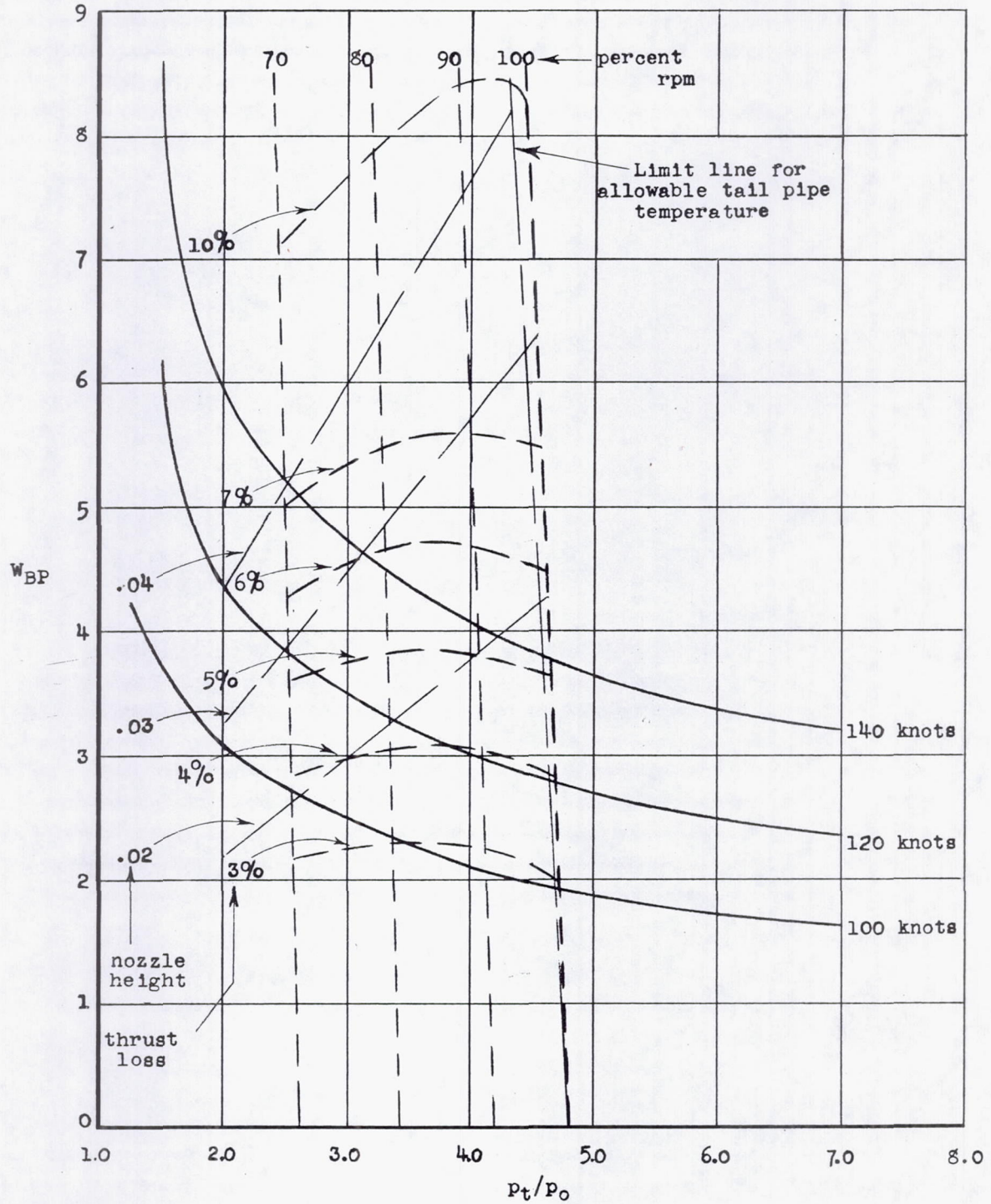


Figure 17.- Comparison of flow and pressure-ratio requirements of blowing flaps, compressor air bleed available from J-47 engine, and performance of various flap nozzles; $\delta_f = 60^\circ$, $C_\mu = 0.012$.

NACA - Langley Field, Va.